Article type: Research Paper

Title: Physical-biological interactions underlying the connectivity patterns of coral-dependent fishes around the Arabian Peninsula

Running title: Biophysical model of reef fishes

Authors (names, affiliation, e-mail addresses):

Felipe Torquato[(1)*], felipe.torquato@qu.edu.qa (correspondence author)

Peter R. Møller[(2,3)], pdrmoller@snm.ku.dk

(1) *Department of Biological and Environmental Science, College of Arts and Sciences, Qatar University, Doha, Qatar.*

(2) *Section for Evolutionary Genomics, Natural History Museum of Denmark, University of Copenhagen, Denmark.*

(3) *Norwegian school of Fisheries, UiT Norwegian Arctic University, Tromsø, Norway*

Acknowledgements

The author F.T. is supported by a CNPq/Brazil fellowship through the programme Science Without Borders (Proc. 232875/2014-6). We also thank Dr Robert Cowen (Oregon University) and Dr Luiz Rocha (California Academy of Sciences) for their helpful comments. No permits were required to conduct this study.

ABSTRACT

Aim: Distribution patterns on lineages alone do not explain the processes underlying phylogenetic differentiation in fishes observed around the Arabian Peninsula, whose hypotheses traditionally rely on either (i) Pleistocene vicariance events, (ii) successive bottlenecks, (iii) recent founder effect, (iv) and large spatial gradients in physical conditions. In this study, we test the hypothesis that phylogeographic patterns of coral-dependent fish species inhabiting the peninsula may be driven by a combination of ocean circulation, larval behavior and seascape features.

Location: Arabian Peninsula.

Taxa: Multitaxa.

Methods: A biophysical modeling system that relies on stochastic Lagrangian framework and Individual-Based Model was used to simulate larval dispersal through three putative barriers, by tracking three-dimensional movements of virtual particles in ocean circulation scenarios. We explored the range of dispersal capabilities across reef fish species by creating 72 hypothetical strategies, each representing a unique combination of five biological traits, namely: pelagic larval duration, spawning periodicity, mortality rate, reproductive output and vertical migration.

Results: The strength of the barriers was highly variable as a function of all biological traits (except reproductive output) and indicated high asymmetry of connectivity, and hence gene flow, between adjacent areas. In addition, direction and distance travelled by the virtual larvae varied according to both the geographic position of releasing site and biannual monsoonal winds. On average, larvae released during the summer exhibited a higher potential for dispersal than larvae released during the winter.

Main conclusions: Our biophysical models showed that in the Arabian Peninsula, the combination of hydrodynamic, seascape features and larval traits likely affect the distribution of genetic lineages due to the interruption, reduction or asymmetry of larval movements through the putative barriers.

KEYWORDS: Biophysical modeling, Connectivity modeling system, Larval dispersal, Oceanographic barriers, Phylogeography.

INTRODUCTION

For coral-dependent organisms, whose populations inhabit discrete habitats, inter patch dispersal occurs mainly during early larval stages when broad spawning sedentary adults release in the water column tiny planktonic propagules, which disperse in association with oceanic current systems. As such, the direction and magnitude of prevailing currents can result in two general scenarios; spread out lineage distribution by aiding the dispersal of the propagules to future patches or hindrance of lineage distribution by disrupting propagules movement. Thus, dispersal mechanisms play a primary role in determining

levels of gene flow in populations, where the first scenario suggests species with high genetic homogeneity across vast areas (i.e., panmintic unit), while the second scenario explains either genetic discontinuities (Bowen et al., 2016) or, ultimately, the existence of endemic species (Cowen et al., 2000).

However, the dispersal in the marine realm is not controlled by ocean circulation alone. Propagules behavioral capabilities create a wide variety of physical-biological interactions that may also maximize or minimize the larval dispersal (Leis, 2020; North et al., 2009). For instance, ontogenetic vertical shift may place the larvae under the influence of different water masses (Stenevik et al., 2003; Torquato & Muelbert 2014), and longer time from hatching to settlement may confer greater dispersal ability (Leis, 2021). In addition, mesoscale oceanographic processes such as fronts (Galarza et al., 2009), river runoffs (Rocha, 2003) and upwelling (Lett et al., 2007), act as semi-permeable barriers to marine faunal connectivity and their permeability are affected by biological traits (Ayre et al., 2009).

In the Arabian Peninsula, zoogeographic and population genetic studies on coral-dependent fishes have shown discontinuities (i.e., barriers) in both species and genetic distributions, respectively, along the seas bordering the peninsula (Berumen et al. 2017; Burt et al., 2011; DiBattista, Roberts, et al., 2016). The most remarkable of these discontinuities is due to the upwelling off Oman, which distinguishes the fish fauna from each side of the peninsula (DiBattista, Choat, et al., 2016). Two other discontinuities in species compositions are observed, one between the Red Sea and the adjacent Gulf of Aden, through the Bab el-Mandeb Strait, and another between the Arabian/Persian Gulf (henceforth referred as the Gulf) and the adjacent Sea of Oman, through the Strait of

Hormuz (DiBattista, Roberts, et al., 2016). These boundaries described by multispecies distribution records, are also logical places to present-day barriers for gene flow between populations (Baums et al., 2006). Indeed, population genetic studies carried out in the Northwestern Indian Ocean (NIO) have revealed similarities in the geographic position of barriers previously proposed (DiBattista et al., 2013, 2015, 2017; Nanninga et al., 2014; Priest et al., 2016; Saenz-Agudelo et al., 2015; Torquato et al., 2019).

Hypotheses to explain the distribution of genetic diversity in the Arabian Peninsula usually rely on either parapatric speciation pattern, which resulted from repeated historical vicariance events or ecological speciation which is due to the large spatial gradients and temporal fluctuations in physical conditions across the peninsula (DiBattista, Roberts, et al., 2016; DiBattista, Choat, et al., 2016; Nanninga et al., 2014). An alternative hypothesis has been attributed to the seasonal upwelling in the Arabian Sea off Oman, which creates unsuitable condition for discrete coral-habitat growth along southern Omani coast (Sheppard & Salm, 1988) and hence potentially restricting stepping-stone connectivity between both sides of the Arabian Peninsula. In turn, little attention has been given to test hypotheses where the combination of seascape features, ocean circulation and larval traits underling the genetic patterns observed among coral-dependent fishes inhabiting the Arabian Peninsula.

Although a more comprehensive picture is emerging in the Arabian Peninsula with respect to marine phylogeographic patterns (Berumen et al., 2017; DiBattista, Roberts, et al., 2016; DiBattista, Choat, et al., 2016), the processes affecting larval dispersal across the putative barriers are not yet fully understood due to the paucity of empirical studies (Berumen et al., 2017; Kemp, 1998). However, in many cases, hypotheses in marine

ecology are prohibitively time-consuming and expensive to be empirically tested, largely due to the impossibility of capturing the full range of temporal and spatial fine-scale resolution required for making inferences (Cowen & Sponaugle, 2009). In addition, political realities of some countries bordering the Western Indian Ocean (WIO) have limited access to scientists, hindering a more thorough investigation of phylogeography pattern in the region (Berumen et al., 2017). In such cases, if limited empirical data are available, reliable computational models can be used to make field predictions and advance our knowledge of designing future experiments for hypothesis testing (Cowen & Sponaugle, 2009).

Advances in physical circulation models have enabled the investigation of population connectivity by running semi-realistic simulations of virtual particles. Here we used high-resolution ocean circulation model (Hybrid Coordinate Ocean Model - HYCOM) to design a biophysical model in a Lagrangian stochastic scheme (Paris et al., 2013). The main goal of this study is to simulate multitaxon larval dispersal through the putative marine barriers, and thus providing insights into processes and patterns of connectivity leading to the distribution of genetic diversity of coral-dependent fishes around the Arabian Peninsula. Specifically, we shed light on three questions: (1) what biological attributes affect the larval dispersal through the Bab el-Mandeb Strait and Strait of Hormuz? (2) What is the impact of the upwelling off Oman on the larval connectivity between both sides of the peninsula? (3) How does oceanographic variability, due to the seasonal monsoon, affects larval dispersal pattern (i.e. direction and magnitude travelled by the particle)? Our results provide detailed predictions that can be compared to previous and future empirical studies on the distribution of biodiversity in the Arabian Peninsula.

MATERIAL AND METHODS

Study area

The Arabian Peninsula lies on a hyper-arid region in Southwest Asia at the junction of this continent with Africa (Figure 1). The water-mass distribution and upper-ocean circulation surrounding the peninsula change in correspondence with biannual wind reversals, creating seasonality in oceanographic conditions (Cutler & Swallow, 1984; Shetye et al., 1994). During the NE monsoon in the winter (November - March), the wind blows away from the Asian continent, and the ocean surface circulation in the Arabian Sea is approximately counter-clockwise. On the other hand, during the summer SW monsoon (May-September), the wind reverses and blows strongly, such that the circulation in the Arabian Sea becomes clockwise. March-April and October, in turn, are transition periods and the winds are weak (see Cutler & Swallow, 1984).

Biophysical model and larval dispersal simulation

Idealized dispersal of fish larvae was modeled using an open-source program, Connectivity Modeling System (CMS v. 2.0; Paris et al., 2013), which is a biophysical modeling system based on stochastic Lagrangian framework and Individual-Based Model (IBM) that couple ocean current, GIS-based habitat, and biological traits. In brief, CMS uses information on currents and environmental conditions to simulate both deterministic fourth-order Runge-Kutta and/or stochastic displacements of numerous virtual particles (hereafter called larvae), through space and time.

The Lagrangian three-dimensional method is a more realistic approach to simulate larval dispersal in comparison to the Eulerian advection-diffusion methods. Additionally,

the Lagrangian approach is more suitable for this study, which aims to assess biological-physical interactions and hydrographic variability conditions (e.g., extreme events, perturbation, instability) on larval dispersal. Nevertheless, although more realistic, Langragian models have computational requirements that make it impossible to release a real number of larvae per species. Alternatively, Eulerian advection-diffusion methods, though not spatially realistic, have a large impact on dispersal kernel and hence are suitable in quantifying evolutionarily significant tails in evolutionary connectivity studies (Treml et al., 2012).

Hydrodynamic model

We used the CMS package *getdata* to download three-hourly ocean current velocities from the three-dimensional and eddy-resolving Hybrid Coordinate Ocean Model (HYCOM, GLBv0.08) from 2018 to 2019. The model had a horizontal resolution of ca. 9 km grid (1/12˚), and was set up in a nested domain (0˚ - 30˚ N, 31˚ - 70˚ E), comprising twenty layers from the surface up to 100 meters depth (see Figure S1.1 – S1.3 in Supporting Information). The HYCOM model has been extensively used in the study area, including the Arabian Sea (McClean, 2015), the Gulf (Yao & Johns, 2010) and the Red Sea (Chang et al., 2008), and is in agreement with other hydrodynamic models (e.g., MIKE 3 FM; Cavalcante et al., 2020).

GIS-based Seascape module

The GIS served to delineate the source and recruitment habitats. Suitable releasing (source habitat) and settlement (sink habitat) locations were delineated in QGIS v.2.18 by

creating a vector grid that overlies the distribution of coral reefs data from the UNEP-WCMC (2010) across the nested domain. Thus, a total of 181 polygons (~ 18km x 18km) representing coral reef habitats were placed along coastal areas within our model domain. It should be noted that we included all the reef areas from the Gulf of Aden, Arabian Sea and Sea of Oman; however, within the Red Sea and the Gulf, only those reefs surrounding the Bab el-Mandeb Strait and the Strait of Hormuz were included, respectively. Reefs positioned too far from the straits were excluded from the model, as the larvae released from them did not reach the putative barriers (see Figure S1.4 in Supporting Information).

Particle-tracking module

Stochastic IBM Lagrangian model tracked offline over 157 million larvae around the Arabian Peninsula for 72 hypothetical strategies (see below). A total of 86,011,200 larvae were released to mimic taxa spawning throughout year, whereas 35,838,000 larvae were tracked to simulate taxa spawning on either winter monsoon (November 2018 – March 2019) or summer monsoon (May 2019 – September 2019).

Preliminary sensitive analysis showed no significant difference in the settlement proportion when seeding 100 larvae from the center of the 181 polygons every 3, 6, 12 or 24 hours (see Appendix S2 in Supporting Information). Therefore, the 100 larvae were released from each reef at every 24 hours, which represented a spawning event. This uniform temporal distribution of larvae allowed us to assess the effects of the hydrographic variability conditions on larval dispersal (e.g., extreme events, perturbation, and instability). The position of each larva was updated every 3 h time-step, and the trajectory information (i.e. longitude, latitude, depth) was saved to output every time-step. We

208 accounted for diffusive turbulent motion by adding a horizontal diffusion coefficient. The
209 value of 50 $m^2.s^{-1}$ was chosen from a sensitivity test where 100 larvae were released from
210 the 181 polygons at every 24 hours (see Appendix S2).
211
212 *Biological module*
213 In order to explore the range of dispersal capabilities across reef fishes, we created
214 72 hypothetical strategies each of those representing a unique combination of five
215 biological traits that may influence the connectivity, namely: pelagic larval duration (PLD),
216 spawning periodicity, mortality rate, reproductive output and vertical migration (Table 1):
217
218 i) Pelagic larval duration (PLD): Herein PLD is defined as the time from larval release to
219 the settlement. After being released, the larvae were left to drift for over a period of 20, 30
220 or 40 days, corresponding to the typical PLD of most coral reef fish species/families
221 (Lindeman et al., 2005; Thresher & Brothers, 1985). In this study, the PLD was equally
222 divided into the three ontogenetic larval stages, namely: preflexion, flexion and
223 postflexion. During the postflexion stage, the larvae were considered competent to settle if
224 they were inside one of the 181 reef sites.
225
226 ii) Larval mortality: Little is known regarding larval mortality in the oceans. To
227 accommodate this uncertainty, our study included two levels of mortality based on the half-
228 life, such that approximately 50% of unsettled larvae would be surviving after half the
229 maximum PLD (Holstein et al., 2014; Paris et al., 2013). Thus, we determined that in high

mortality scenarios, about half of the larvae died by the end of the preflexion stage, while in low mortality condition half of the larvae died by the end of the postflexion stage.

iii) Vertical migration: Due to the paucity of basic data regarding fish larvae distribution within our study area, the model incorporated an idealized pattern of ontogenetic vertical migration for the three larval stages (see Figure S1.5 in Supporting Information). This idealization assumed the existence of a global trend of the fish larvae to display downward ontogenetic shift in vertical distribution (Irisson et al., 2010). In order to assess the importance of vertical migration, we contrasted both epipelagic ichthyoplankton moving only horizontally along the sub-surface layer and larvae that, besides the horizontal displacement, also moved vertically according to its ontogeny.

iv) Reproductive output: We assumed spatial homogenous reproductive output among the habitats, whereby all the 181 polygons were set to release the same number of larvae per 'spawning' event. However, we contrasted scenarios where reproductive output varies among species. In scenarios of high reproductive output, a hundred larvae were released from each polygon at every spawning event, whereas in low reproductive output conditions, only ten larvae were released per event.

v) Spawning periodicity: Three seasonal spawning preferences were accounted by simulating the larval dispersal annually and according to the two dominant seasonal oceanographic conditions around the Arabian Peninsula, namely, winter (November - March) and summer (May - September).

Analyses

The proportion of survivor larvae that were released from each region *i* and successfully settled in a downstream habitat patch (i.e., sink habitat) at region *j*, was plotted as a connectivity matrix. The diagonal of the matrix represents the local retention, i.e., the fraction of all larvae produced at a focal patch returning to that patch (Botsford et al., 2009). In order to evaluate the strength and direction of the potential connections on regional scales (e.g., between Red Sea and Gulf of Aden), all cells from each region were merged.

Biological traits vs. biogeographic barriers

The effects of both Bab-el-Mandeb and Hormuz strait were measured in terms of permeability, which herein is considered as the proportion of surviving larvae that were released from a source habitat, passed through the strait, and successfully settled on the other side. In turn, the effect of the upwelling off Oman was measured in terms of local retention proportion along the Arabian Sea. At this region, we hypothesized that the upwelling acts as a barrier because the Ekman transport tends to displace the larvae toward offshore, where suitable habitats for settlement are not available. Therefore, we assumed that a higher local retention represents a greater chance of connectivity since the larvae moving along the coast will be retained on the continental shelf where the suitable reef habitat is found (but see Morgan et al., 2012). In contrast, a lower local retention decreases the chance of connectivity, as the larvae moving offshore will not settle before their critical period.

To evaluate the effect of the biological traits highlighted in Table 1 on the strength of the putative barriers, we relied on an extended approach of Generalized Linear Models (GLMs) in R-studio v.4.1.0 (R Development Core Team, 2008). Given that the above mentioned proportion is a continuous variable taking on values restricted to the interval between 0 and 1, we used a beta regression model as proposed by Ferrari & Cribari-Neto (2004) through the 'betareg' R-package (Cribari-Neto & Zeilis, 2010). The beta regression shares many similarities with GLMs, yet differ with respect to how parameters are estimated (Douma & Weedon, 2019). The model essentially describes the relationship between the response variables Y_i (hereby, proportions), and the predictors X_i (Table 1) through a linear predictor η_i. This linear predictor is then linked to the mean of the response $E(Y_i) = \mu_i$ by using a link function g, such that $g(\mu_i) = \eta_i$. Thus, the applied model can be summarized as:

$$Y_i \sim B(\mu_i, \phi)$$

$$\text{logit}(\mu_i) = \eta_i$$

$$\eta_i = \beta_0 + \beta_1 PLD + \beta_2 SP + \beta_3 M + \beta_4 R + \beta_5 VM + \varepsilon$$

Where ϕ is the precision parameter; η_i the linear predictor expressed on a logit scale; $\beta 0$ the intercept; $\beta 1$-5 the repressors related to each explanatory variable (PLD=Pelagic larval duration, SP = Spawning periodicity, M = Mortality, R = Reproductive output, VM = Vertical migration); and ε represents the error term.

Pairwise comparison of significant factor levels ($p < 0.05$) containing more than two levels was then applied through the Tukey's post-hoc test. To do so, we used the *glht*

function from the 'multcomp' R-package (Hothorn et al., 2008). Model quality was assessed through residual diagnostic plots as suggested by Zuur et al. (2010). Normality was evaluated by means of Quantile-Quantile plots, while homogeneity was assessed by contrasting the residuals against the predicted values. Finally, the coefficient of determination (R^2) was used to check for model fit, where values close to 1 are indicative of good predictive quality.

Larval dispersal pattern and oceanographic conditions

The maximum distances travelled by the larvae around the Arabian Peninsula were calculated by setting up a model with the lowest mortality rate and40-day PLD. We used the program QGIS to measure this distance and compare the results between summer and winter, as well as in each of the regions within the model domain.

RESULTS

Effects of the biological traits on the permeability of biogeographic barriers

Five different Beta regressions were conducted to evaluate the effects of the biological traits on the permeability of the biogeographic barriers highlighted in Figure 1. However, for both Bab-el-Mandeb and Hormuz straits, two models were fit to evaluate the effects in each direction, only one model was fit for the barrier off Oman as a means of testing for local retention.

The graphical evaluation of the model assumptions revealed that all tested models fit well to the simulated data, with residuals following both homoscedasticity and normality assumptions, and with R^2-values ranging between 0.73 and 0.94. Tables S3.1-S3.3 in

Supporting Information summarize the numerical outputs of all Beta regressions, which also corroborate with our simulations. Below we discuss in more detail the obtained results according to the evaluated biological traits.

i) Pelagic larval duration (PLD): In both directions through the Bab el-Mandeb Strait, the permeability was not altered as the PLD changed (Figure 2). On the other hand, in the Strait of Hormuz, the chances of the larvae released in the Gulf to successfully settle on the reefs in the Sea of Oman, and vice-versa, was higher when the larvae drifted for 40 days compared to when it drifted for 20 days. No difference though was found between 30 days and 20 days, or between 30 days and 40 days. In the Arabian Sea, the highest larval retention, and hence the highest chance of connectivity, occurred with the lowest PLD (i.e., 20 days). In addition, the proportion of larval retention in this region did not change between 30- and 40-day-PLD (Figure 4).

ii) Larval mortality: The mortality rate demonstrated a negative relationship with permeability across both straits. Therefore, the resistance to larval movement through the Bab el-Mandeb Strait and the Strait of Hormuz increased as the mortality rate decreased (Figures 2 and 3). In the same vein, in the Arabian Sea, the local retention of larvae was higher when the mortality rate had its lowest value (Figure 4).

iii) Vertical migration: The ontogenetic vertical movement influenced the permeability of the barriers along the Arabian Peninsula. In both directions across the Bab el-Mandeb Strait, the larvae significantly decreased their permeability when they performed vertical

migration (Figure 2). In the Strait of Hormuz, the vertical migration increased the larval movement from the Gulf to the Sea of Oman, but constrained the movement in the opposite direction (Figure 3). In the Arabian Sea, this biological trait had no impact on the local retention of larvae (Figure 4).

iv) Reproductive output: No significant difference was observed for distinct reproductive outputs. Varying the number of larvae released from a source region during each spawning event, had no effect on the proportion of larvae that crossed either straits (Bab el-Mandeb Strait or Strait of Hormuz) and successfully settled on the adjacent sea (Figures 2 and 3). In the same vein, distinct reproductive outputs did not change significantly the proportion of larvae that was retained onshore along the Arabian Sea (Figure 4).

v) Spawning periodicity: The spawning season influenced the permeability of the barriers. The larvae that were released from the Gulf of Aden and settled on the Red Sea increased their success of connection during the winter relative to the summer. On the contrary, in the opposite direction, the permeability was higher in the summer compared to winter (Figure 2). In the Strait of Hormuz, neither the proportion of larvae leaving the Gulf nor the proportion of larvae settling in the Sea of Oman changed throughout the year. However, in the opposite direction, this proportion was significantly higher during the winter compared to the summer (Figure 3). In the Arabian Sea, the seasonal spawning did not affect the proportion of larval retention on the continental shelf (Figure 4).

Connectivity matrix

From a total of 72 matrices representing the hypothetical strategies, 70 matrices revealed that connectivity occurred exclusively between neighboring regions, while for two strategies, the larvae released from the Arabian Sea reached the reefs in the Red Sea. No interruptions were found between neighboring regions when the larvae were left to drift for 40 days (see Figure S3.1 – S3.3 in Supporting Information).

In our simulations, the hardest putative barrier was observed in the region off Oman, which separates both sides of the Arabian Peninsula. For 10 strategies, the connection was completely interrupted from the Gulf of Aden to the Arabian Sea, mainly in the summer and when including the vertical migration. For 11 strategies, the larvae released from the Arabian Sea did not reach the Gulf of Aden. It occurred exclusively during the summer and especially for those scenarios without vertical migration. For all strategies, the larvae released from the Sea of Oman always settled on the reefs in the Arabian Sea. However, for 9 strategies, the connection was interrupted from the Gulf of Aden to the Arabian Sea, predominantly during the summer and when the larvae performed vertical migration (Figure S3.1 – S3.3).

Particles trajectories: seasonal variability of spatial scale and direction

The direction and distance travelled by the larvae were highly variable as a function of both the geographic position of releasing site and the biannual monsoonal winds (Figures 5 and 6). On average, larvae released during the summer exhibited a higher potential for dispersal, especially in areas that are not enclosed (Figures 5f and 6f). It was in the summer that the southward movement of larvae from the Red Sea was more pronounced, and it was

390 also in this season that numerous larvae released in the Gulf of Aden reached Omani waters
391 in the Arabian Sea. In turn, during the winter, the vast majority of larvae originating in the
392 Red Sea were retained within this area, while larvae released within the Gulf of Aden either
393 moved eastward, though rarely reaching the Omani coast, or moved southward along the
394 Somali coast.

395 In the Arabian Sea, surface circulation exhibited a strong seasonal cycle. During
396 the summer, larvae released along the Omani coast between 54.6˚ E and 56.1˚ E, either
397 moved eastward alongshore toward the Sea of Oman or sharply turned toward the open
398 ocean. However, larvae released between 57.8˚ E and 59˚ E were exclusively transported
399 alongshore toward the Sea of Oman (Figure 5c). In the winter, even though the larvae along
400 the entire Omani coast moved toward offshore, on average, they travelled shorter distances
401 relative to the summer (Figures 5f and 6f).

402 On the east side of the Arabian Peninsula, the temporal variability of both the
403 direction and the distance travelled by the larvae was less evident. In the Sea of Oman,
404 larvae released from the eastern Omani coast tended to move southward in both seasons.
405 However, especially in the summer, those larvae originating from the top of the Sea of
406 Oman were able to pass through the Strait of Hormuz. In the Gulf, the patterns of dispersal
407 observed in both seasons were quite similar, larvae tended not to move far away and hence
408 most of them remained in the Gulf.

409

410 **DISCUSSION**

411 Measuring the strength of barriers has been a great challenge to the understanding
412 of phylo- and bio-geographic patterns (Treml et al., 2015). In the present study, a series of

413 individual-based simulations were performed to assess the permeability of larvae of 72
414 different combinations of five key biological parameters through three putative barriers.
415 This 'multitaxa' comparison demonstrated how physical-biological interactions determine
416 the success of propagules being transported through the Bab el-Mandeb Strait and the Strait
417 of Hormuz, as well as of those being retained on the continental shelf off Oman. Here, we
418 hypothesized that coupling hydrodynamic, seascape features and larval traits, potentially
419 contribute to the connectivity/gene flow and hence to the distribution of genetic lineages.
420 Therefore, we assumed that the absence, strong reduction or asymmetry of larval exchange
421 through the putative barriers, affect the phylogeographic pattern around the Arabian
422 Peninsula.

423 Unfortunately, there is a paucity of data on the biological traits for the species
424 inhabiting the study area, especially those data related to vertical distribution of larvae,
425 mortality rate and reproductive output. Thus, the hypotheses presented in our study will be
426 mainly discussed according to the PLD and the spawning time (based on either
427 ichthyoplankton survey or gonadal maturity stage), when this information exists for the
428 species whose phylogeographic study was carried out in the Arabian Peninsula.

429

430 **Biological traits and empirical (genetic) evidences**

431 The hardest putative barrier observed in the connectivity matrices was that
432 positioned off Oman, with scenarios exhibiting weak or no connectivity between the
433 Arabian Sea and its adjacent areas. This result corroborates with previous empirical
434 population genetic studies. For example, phylogeographic investigations on fish species,
435 such as *Scomberomorus commerson* (van Herwerden et al., 2006); *Cephalopholis*

436 *hemistiktos* (Priest et al., 2016); *Pomacanthus maculosus* (Torquato et al., 2019);
437 *Ctenochaetus striatus* and *Chaetodon trifascialis* (DiBattista et al., 2020), using different
438 molecular methods, found a sharp genetic discontinuity positioned in southern Oman,
439 although *S. commerson* is not a coral-dependent species.

440 Although the beta regression model did not exhibit a significant effect on the
441 spawning time on the local retention, the matrices showed that the connectivity between
442 the Arabian Sea to the Gulf of Aden, and vice-versa, as well as from the Arabian Sea to the
443 Sea of Oman were completely interrupted in some scenarios during the summer monsoon.
444 This prediction is in line with the gonado-somatic index (GSI) values for the three first
445 species mentioned above, i.e., *S. commerson* (Kaymaram et al., 2010); *C. hemistiktos*
446 (Priest et al., 2016) and *P. maculosus* (Grandcourt et al., 2010), which indicate that they
447 spawn mainly in the summertime. Regarding the PLD, the connectivity between the
448 Arabian Sea and adjacent regions was interrupted in some scenarios of both 20 and 30-
449 PLD, but never for those that the larvae drifted for 40 days. Among the coral-dependent
450 species, the PLD for *Cephalopholis* has not been determined, but a 40-day average is
451 proposed for the subfamily Epinephelinae (Lindeman et al., 2001). However, *Pomacanthus*
452 species usually have a short (~ 17–24 days) PLD (Thresher & Brothers, 1985).

453 All the 72 combinations used in our simulations showed connectivity from the Red
454 Sea to the Gulf of Aden, and vice-versa. Although there is high level of endemism within
455 the Red Sea (DiBattista, Roberts, et al., 2016), investigations carried out hitherto have not
456 shown genetic discontinuities for fish coral-dependent species through the Bab el-Mandeb
457 Strait. The genetic studies include *Amphiprion bicinctus* (Saenz-Agudelo et al., 2015),
458 *Mulloidichthys f. flavolineatus* (Fernandez-Silva et al., 2016), *C. hemistiktos* (Priest et al.,

2016), *P. maculosus* (Torquato et al., 2019), *Ctenochaetus striatus* and five *Chaetodon* spp. (DiBattista et al., 2020), as well as sea anemones (Emms et al., 2019). Our biophysical models indicated that the chance of the larvae being released in the Red Sea and settle in the Gulf of Aden increases during the summer. Ichthyoplankton surveys carried out in the Red Sea showed that the vast majority of fish taxa inhabiting the region, such as *A. bicinctus* (El-Regal, 2013), spawn mainly during spring and summer. In addition, the GSI of *M. flavolineatus* is higher during this season, and its larval peak densities occur in August (El-Regal, 2018). The models also revealed that the PLD did not impact the permeability through the Bab el-Mandeb Strait, what can explain the lack of genetic discontinuity even for species with short PLD such as *A. bicinctus* (Saenz-Agudelo et al., 2015).

In fact, the strength of the Bab el-Mandeb Strait has been mainly supported by the species distribution studies, and Kemp (1998) suggested that the strait does not act as a present-day barrier. According to the author, the paucity of information about the reef fish assemblage inhabiting the southern Red Sea and the adjacent Gulf of Aden is the main reason for the hypothesis supporting that the strait acts as a present-day barrier (see Berumen et al., 2017).

On the other side of the peninsula, genetic data have shown that for coral-dependent fish species, such as *C. hemistiktos* (Priest et al., 2016), *Nemipterus japonicus* (Farivar et al., 2017), *P. maculosus* (Torquato et al., 2019) and *Istiblennius pox* (Mehraban et al., 2020), the Gulf and the Sea of Oman represent a single phylogeographic province. However, a phylogeographic study of *Periophthalmus waltoni*, a marine amphibious fish with terrestrial adaptations, revealed two distinct genetic clusters, one represented by the

Gulf individuals and the other by individuals from the Sea of Oman. Likewise, genetic investigations involving corals (Howells et al., 2016; Torquato et al., 2021) and sea urchin (Ketchum et al., 2020) showed a genetic discontinuity through the Strait of Hormuz. Indeed, biogeographic survey indicated higher levels of endemism for invertebrates within the Gulf compared to fishes (DiBattista, Roberts, et al., 2016).

Our models showed that the strongest connectivity from the Sea of Oman to the Gulf occurred during the winter, but the spawning time does not impact the connectivity from the Gulf to the Sea of Oman. Investigations on the temporal patterns of reproduction of *Platygyra daedalea* and *Acropora downingi* revealed that both species spawn mainly between March and May (Bauman et al., 2011), during the transition periods when the winds are weak (Cutler & Swallow, 1984). Additionally, our model showed that high mortality rate in the first third of the PLD increases the strength of the barrier. Experiments with *Acropora* showed that its larval survival strongly declined after the first few days after spawning, with half-life shorter than 5 days (Graham et al., 2008). Nevertheless, the population differentiation of *P. daedalea* and *A. downingi* through the Strait of Hormuz, have also been explained by natural selection (Howells et al., 2016) and recent bottlenecks (Torquato et al., 2021), respectively. In turn, the sea urchin (*Echinometra* sp.), which also exhibited the genetic discontinuity through the strait, spawns in June (Alsaffar & Lone, 2000) and the PLD within the genus varies from 18 to 30 days (McClanahan & Muthiga, 2007). This combination agrees with the biophysical models since the connectivity from the Sea of Oman to the Gulf decreases during the summer, especially with low PLD.

Putative barriers: our finds and previous hypotheses

The main hypotheses to explain genetic differentiation between both sides of the peninsula usually involve seascape features and/or ocean circulation off Oman (Torquato et al., 2019). In the southern Omani coast, the seascape is characterized by weakly developed coral colonies that are represented by a reduced number of species (Burt et al., 2016; Sheppard & Salm, 1988). Hence, the lack of coral-habitat creates an unbridgeable gap for coral-dependent species moving through the continental shelf of the Arabian Sea (Priest et al., 2016). In turn, the ocean circulation explanation relies on studies carried out in other regions, which suggest that upwelling systems hinder connectivity along the continental shelf by displacing larvae offshore due to the Ekman transport (Parrish et al., 1981; but see Morgan et al., 2012). For coral-dependent species, this is particularly relevant since reef habitats are solely located in onshore areas. Therefore, the larvae moving to offshore areas will not find suitable habitats for settlement before the end of their critical period. Another hypothesis involving the ocean circulation in the Omani coast is an intense offshore jet formed during the summer monsoon near the Ras al Hadd cape, between the Sea of Oman and the Arabian Sea (Ayouche et al., 2021).

Besides the seascape features and the ocean circulation, cold water displaced from the sea bottom to the surface during upwelling events may also affect the survival of larvae and alter their behavior. At peak upwelling in summer, sea surface temperatures off Oman is often below 20°C (Elliott & Savidge, 1990; Claereboudt, 2019). Furthermore, the cold-water upwelling in the Arabian Sea and the warm waters of the Sea of Oman create a thermal front between both seas, off Ras al Hadd cape (Ayouche et al., 2021). Additionally, the cold water along southern Oman may hinder the dispersal of larvae intolerant to low

temperatures (Fleminger, 1986). Furthermore, larvae in colder water grow slower (Rankin & Sponaugle, 2011), and according to the growth-mortality hypothesis (Anderson, 1988), the chances of the larvae escaping attack by predators increase with increasing growth rate. Therefore, the connectivity between both sides of the peninsula may be affected by cold water as mortality increases.

Regarding the straits, our biophysical models showed an asymmetric movement through both the Bab el-Mandeb Strait and the Strait of Hormuz. The asymmetry of the former is in accordance with a combination of the seasonal water exchange pattern between the Red Sea and Gulf of Aden, and vertical movements. The water flowing through the Bab el-Mandeb Strait changes from a two-layer surface flow in the winter to a three-layer flow in the summer (Smeed, 2004). Thus, the connectivity is affected if the larvae are positioned in one or another prevailing current. A second hypothesis that supports the Bab el-Mandeb Strait as a barrier is related to sea level variation during the Pleistocene glaciation (DiBattista, Choat, et al., 2016), when the water exchange between the Red Sea and the Gulf of Aden was repeatedly interrupted. Besides the period of allopatry, the interruption of water exchange leads to hypersaline condition within the Red Sea, which could favor a differentiation (DiBattista, Choat, et al., 2016).

On the other side of the peninsula, the relatively high evaporation rate over the Gulf combined with the limited water exchange with the open ocean drives an inverse estuarine system at the Strait of Hormuz, with a shallow inflow of the Indian Ocean Surface Water (IOSW) and a deep outflow of the Persian Gulf Water (PGW; Swift & Bower, 2003). The currents in the surface layers are highly variable and exhibit large amplitude variation, mainly in the wintertime (Johns et al., 2003). However, in the spring, the inflow is wider

551 and fills the entire width of the strait (Chao et al., 1992). The outflow in deep layers, in
552 turn, is relatively steady throughout the year with a little seasonal variance (Johns et al.,
553 2003, Swift & Bower, 2003). This pattern in water circulation explains, for example, that
554 the proportion of larvae leaving the Gulf did not change seasonally, and increased when
555 the larvae performed vertical migration. In the opposite direction, epipelagic larvae
556 released in the Gulf of Oman had a higher chance to reach the Gulf, especially during the
557 winter when the inflow surface is highly variable.

558 The limited water exchange with open-ocean and the high evaporation rate also
559 create extreme environment conditions within the Gulf region. Besides the hypersaline
560 water (often > 42 ppt; Swift & Bower, 2003), during the summer, the sea surface
561 temperature is usually > 35 ˚C and makes this body of water the warmest sea on the Earth
562 (Vaughan et al., 2019). This extreme condition presumes intense natural selection, such
563 that strong signatures (i.e., high frequency) of heat tolerant alleles, for example, are
564 predicted across the genome. Therefore, both reduction and asymmetry of migration rate
565 through the Strait of Hormuz and the strong natural selection due to the extreme
566 environment conditions are indeed expected to be observed along the peninsula.

567 The Pleistocene also created conditions to differentiate populations between the
568 Gulf and the Sea of Oman (Torquato et al., 2021). During the glacial maxima, when the
569 sea level lowered at 120 m than the present, the Gulf had its ground almost completely
570 espoused. Nevertheless, 15000 years ago, this basin started receiving IOSW through the
571 Strait of Hormuz such that the modern shorelines in the Gulf developed ca. 3000–6000
572 years ago (Lambeck, 1996; Vaughan et al., 2019). Thus, the populations currently
573 inhabiting this sea were established only in the last few millennia. This scenario of recent

574 founded effect combined with the restricted gene flow between the Gulf and its adjacent
575 Sea of Oman, is one of the hypothesis to explain the phylogeographic pattern observed in
576 the region (Torquato et al., 2021).
577

578 Data availability statement

579 The model output data yielded in this manuscript are available from the Zenodo repository
580 at https://doi.org/10.5281/zenodo.5814688. The reef distribution data used to design the
581 GIS-based seascape module were obtained from UNEP-WCMC (2010), available at http://
582 https://data.unep-wcmc.org/datasets/1. The oceanographic data (u-velocity and v- velocity)
583 used in the biophysical dispersal model were downloaded from the HYCOM+NCODA
584 Global 1/12° Analysis available at https://www.hycom.org/data/glbv0pt08/expt-93pt0.
585

586 References

587 Alsaffar, A. H. & Lone, K. P. (2000). Reproductive cycles of *Diadema setosum* and
588 *Echinometra mathaei* (Echinoidea: Echinodermata) from Kuwait (northern
589 Arabian Gulf). *Bulletin of Marine Science*, 67, 845-856.
590 Anderson, J. T. (1988). A review of size dependent survival during pre-recruit stages of
591 fishes in relation to recruitment. *Journal of Northwest Atlantic Fishery Science*, 8,
592 55–66.
593 Ayouche, A., De Marez, C., Morvan, M., L'Hegaret, P., Carton, X., Le Vu, B., & Stegner,
594 A. (2021). Structure and dynamics of the Ras al Hadd oceanic dipole in the Arabian
595 Sea. *Oceans*, 2, 105-125.
596 Ayre, D. J., Minchinton, T. E., & Perrin, C. (2009). Does life history predict past and
597 current connectivity for rocky intertidal invertebrates across a marine
598 biogeographic barrier? *Molecular Ecology*, 18, 1887–1903.
599 Bauman, A. G., Baird, A. H., & Cavalcante, G. H. (2011). Coral reproduction in the world's
600 warmest reefs: southern Persian Gulf (Dubai, United Arab Emirates). *Coral Reefs*,
601 30, 405-413.
602 Baums, L. B., Paris, C. B., & Chérubin, L. M. (2006). A bio-oceanographic filter to larval
603 dispersal in a reef-building coral. *Limnology and Oceanography*, 51, 1969-1981.
604 Berumen, M. L., DiBattista, J. D., & Rocha, L. A. (2017). Introduction to virtual issue on
605 Red Sea and Western Indian Ocean biogeography. *Journal of Biogeography*, 44,
606 1923–1926.

Botsford, L. W., White, J. W., Coffroth, M. A., Paris, C. B., Planes, S., Shearer, T. L., ... Jones, G. P. (2009). Connectivity and resilience of coral reef metapopulations in marine protected areas: matching empirical efforts to predictive needs. *Coral reefs*, 28, 327-337.

Bowen, B. W., Gaither, M. R., DiBattista, J. D., Iaccheia, M., Andrews, K. R., Grant, W. S., Toonen, R. J., & Briggs, J. C. (2016). Comparative phylogeography of the ocean planet. *Proceedings of the National Academy of Sciences*, 113, 7962–7969.

Burt, J. A., Feary, D. A., Bauman, A. G., Usseglio, P., Cavalcante, G. H., Sale, & P. F. (2011). Biogeographic patterns of reef fish community structure in the northeastern Arabian Peninsula. *ICES Journal of Marine Science*, 68, 1875–1883.

Burt, J. A., Coles, S., van Lavieren, H., Taylor, O., Looker, E., & Samimi-Namin, K. (2016). Oman's coral reefs: A unique ecosystem challenged by natural and man-related stresses and in need of conservation. *Marine Pollution Bulletin*, 105, 498-506.

Cavalcante, G., Vieira, F., Mortensen, J., Ben-Hamadou, R., Range, P., Goergen, E. A., ... Riegl, B. M. (2020). Biophysical model of coral population connectivity in the Arabian/Persian Gulf. *Advances in Marine Biology*, 87, 193.

Chang, Y. S., Özgökmen, T. M., Peters, H., & Xu, X. (2008). Numerical simulation of the Red Sea outflow using HYCOM and comparison with REDSOX observations. *Journal of physical oceanography*, 38, 337-358.

Chao, S-Y., Kao, T. W., & Al-Hajri, K. R. (1992). A numerical investigation of circulation in the Arabian Gulf, *Journal of Geophysical Research*, 11, 219–236.

Claerbout, M. R. (2019). Oman. In C. Sheppard (Ed.), *World seas: An environmental evaluation* (pp. 25–34). Massachusetts: Academic Press.

Cowen, R. K., Lwiza, K. M. M., Sponaugle, S., Paris, C. B., & Olson, D. B. (2000). Connectivity of Marine Populations: Open or Closed? *Science*, 287, 857-859.

Cowen, R. K., & Sponaugle, S. (2009). Larval Dispersal and Marine Population Connectivity. *Annual Review of Marine Science*,1, 443–466.

Cribari-Neto, F., & Zeileis, A. (2010). Beta Regression in R. *Journal of Statistical Software*, 34, 1–24.

Cutler, A. N., & Swallow, J. C. (1984). Surface currents of the Indian Ocean (to 25S, 100E): compiled from historical data archived by the Meteorological Office, Institute of Oceanographic Sciences.

DiBattista, J. D., Berumen, M. L., Gaither, M. R., Rocha, L. A., Eble, J. A., Choat, J. H., … Bowen, B. W. (2013). After continents divide: comparative phylogeography of reef fishes from the Red Sea and Indian Ocean. *Journal of Biogeography*, 40, 1170 – 1181.

DiBattista, J. D., Waldrop, E., Rocha, L. A., Craig, M. T., Berumen, M. L., & Bowen, B. W. (2015). Blinded by the bright: A lack of congruence between colour morphs, phylogeography and taxonomy for a cosmopolitan Indo‐Pacific butterflyfish, Chaetodon auriga. *Journal of Biogeography*, 42, 1919-1929.

DiBattista, J. D., Roberts, M. B., Bouwmeester, J., Bowen, B. W., Coker, D. J., Lozano-Cortes, D. F., … Berumen, M. L. (2016). A review of contemporary patterns of endemism for shallow water reef fauna in the Red Sea. *Journal of Biogeography*, 43, 423–439.

DiBattista, J. D., Choat, J. H., Gaither, M. R., Hobbs, J. A., Lozano-Cortes, D. F., Myers, R. F., … Berumen, M. L. (2016). On the origin of endemic species in the Red Sea. *Journal of Biogeography*, 43, 13–30.

DiBattista, J. D., Gaither, M. R., Hobbs, J. A., Saenz-Agudelo, P., Piatek, M. J., Bowen, B. W., … Berumen, M. L. (2017). Comparative phylogeography of reef fishes from the Gulf of Aden to the Arabian Sea reveals two cryptic lineages. *Coral Reefs*, 36, 625–638.

DiBattista, J. D., Saenz-Agudelo, P., Piatek, M. J., Cagua, E. F., Bowen, B. W., Choat, J. H., ... McIlwain, J. H. (2020). Population genomic response to geographic gradients by widespread and endemic fishes of the Arabian Peninsula. *Ecology and Evolution*, 10, 4314-4330.

Douma, J. C., & Weedon, J. T. (2019). Analysing continuous proportions in ecology and evolution: A practical introduction to beta and Dirichlet regression. *Methods in Ecology and Evolution*, 10, 1412-1430.

El-Regal, M. A. (2013). Spawning seasons, spawning grounds and nursery grounds of some Red Sea fishes. *The Global Journal of Fisheries and Aqua*, 6, 105-125.

El-Regal, M. (2018). Reproductive biology of the yellow-striped goatfish *Mulloidichthys flavolineatus* (Lacepède, 1801)(Perciformes: Mullidae) in the Red Sea, Egypt. *Egyptian Journal of Aquatic Biology and Fisheries*, 22, 233-247.

Elliott, A. J., & Savidge, G. (1990). Some features of the upwelling off Oman. *Journal of Marine Research*, 48, 319-333.

Emms, M. A., Saenz‐Agudelo, P., Giles, E. C., Gatins, R., Nanninga, G. B., Scott, A., ... Berumen, M. L. (2020). Comparative phylogeography of three host sea anemones in the Indo‐Pacific. *Journal of Biogeography*, 47, 487-500.

Farivar, S., Jalil-Piran, Z., Zarei, F., & Hosseinzadeh Sahafi, H. (2017). Intraspecific phylogeography of the Japanese threadfin bream, *Nemipterus japonicus* (Perciformes: Nemipteridae), from the Persian Gulf and Indo-West Pacific: a preliminary study based on mitochondrial DNA sequence. *Iranian Journal of Fisheries Sciences*, 16(2), 587-604.

Fernandez-Silva, I., Randall, J. E., Golani, D., & Bogorodsky, S. V. (2016). *Mulloidichthys flavolineatus flavicaudus* Fernandez-Silva & Randall (Perciformes, Mullidae), a new subspecies of goatfish from the Red Sea and Arabian Sea. *ZooKeys*, 605, 131-157.

Ferrari, S., & Cribari-Neto, F. (2004). Beta Regression for Modelling Rates and Proportions. *Journal of Applied Statistics*, 31, 799-815.

Fleminger, A. (1986). The Pleistocene equatorial barrier between the Indian and Pacific oceans and a likely cause for Wallace's Line. *UNESCO Technical Papers in Marine Science*, 49, 84–97.

Galarza, J. A., Carreras-Carbonell, J., Macpherson, E., Pascual, M., Roques, S., Turner, G. F., & Rico, C. (2009). The influence of oceanographic fronts and early-life-history traits on connectivity among littoral fish species. *Proceedings of the National Academy of Sciences*, 106, 1473-1478.

Graham, E. M., Baird, A. H., & Connolly, S. R. (2008). Survival dynamics of scleractinian coral larvae and implications for dispersal. *Coral reefs*, 27, 529-539.

Grandcourt, E., Al Abdessalaam, T. Z., Francis, F., & Al Shamsi, A. (2010). Age-based life history parameters and status assessments of by-catch species (*Lethrinus*

borbonicus, *Lethrinus microdon*, *Pomacanthus maculosus* and *Scolopsis taeniatus*) in the southern Arabian Gulf. *Journal of Applied Ichthyology*, 26, 381-389.
Holstein, D. M., Paris, C. B., & Mumby, P. J. (2014). Consistency and inconsistency in multispecies population network dynamics of coral reef ecosystems. *Marine Ecology Progress Series*, 499, 1-18.
Hothorn, T., Bretz, F., & Westfall, P. (2008). Simultaneous inference in general parametric models. *Biometrical Journal: Journal of Mathematical Methods in Biosciences*, 50, 346-363.
Howells, E. J., Abrego D., Meyer E., Kirk N. L. & Burt J. A. (2016). Host adaptation and unexpected symbiont partners enable reef-building corals to tolerate extreme temperatures. *Global Change Biology*, 22, 2702-2714.
Irisson, J. O., Paris, C. B., Guigand, C., & Planes, S. (2010). Vertical distribution and ontogenetic ‘‘migration’’ in coral reef fish larvae. *Limnology and Oceanography*, 55, 909–919.
Johns, W. E., Yao, F., & Olson, D. B. (2003). Observations of seasonal exchange through the Straits of Hormuz and the inferred heat and freshwater budgets of the Persian Gulf. Journal of Geophysical Research, 108, C12, 3391.
Kaymaram, F., Hossainy, S. A., Darvishi, M., Talebzadeh, S. A., & Sadeghi, M. S. (2010). Reproduction and spawning patterns of the *Scomberomorus commerson* in the Iranian coastal waters of the Persian Gulf & Oman Sea. *Iranian Journal of Fisheries Sciences*, 9, 233-244.
Kemp, J. M. (1998). Zoogeography of the coral reef fishes of the Socotra Archipelago. *Journal of Biogeography*, 25, 919–933.
Ketchum, R. N., Smith, E. G., DeBiasse, M. B., Vaughan, G. O., McParland, D., Leach, W. B., ... Reitzel, A. M. (2020). Population genomic analyses of the sea urchin Echinometra sp. EZ across an extreme environmental gradient. *Genome biology and evolution*.
Lambeck, K. (1996). Shoreline reconstructions for the Persian Gulf since the last glacial maximum. *Earth and Planetary Science Letters*, 142, 43-57.
Leis, J. M. (2021). Perspectives on larval behaviour in biophysical modelling of larval dispersal in marine, demersal fishes. *Oceans*, 2, 1-25.
Lett, C., Veitch, J., van der Lingen, C. D., & Hutchings, L. (2007). Assessment of an environmental barrier to transport of ichthyoplankton from the southern to the northern Benguela ecosystems. *Marine Ecology Progress Series*, 347, 247–259.
Lindeman, K. C., Lee, T. N., Wilson, W. D., Claro, R., & Ault, J. S. (2001). Transport of larvae originating in southwest Cuba and the Dry Tortugas: evidence for partial retention in grunts and snappers.
Lindeman, K. C., Richards, W. J., Lyczkowski-Shultz, J., Drass, D. M., Paris, C. B., Leis, J. M., Lara, M., & Comyns, B. H. (2005). Lutjanidae: snappers. In W. J. Richards (Ed.), *Early stages of Atlantic fishes* (pp. 1549–1586). CRC Press.
McClanahan TR, & Muthiga N. A. (2007). Ecology of Echinometra. In J. M. Lawrence (Ed.), *Developments in Aquaculture and Fisheries Science* (pp 297-3170) Elsevier.
McClean, J. L. (2015). Monsoon Variability in the Arabian Sea from Global 0.08 deg HYCOM Simulations. *University of California San Diego La Jolla United States*.
Mehraban, H., Esmaeili, H. R., Zarei, F., Ebrahimi, M., & Gholamhosseini, A. (2020). Genetic diversification, population structure, and geophylogeny of the Scarface

744 rockskipper *Istiblennius pox* (Teleostei: Blenniidae) in the Persian Gulf and Oman
745 Sea. *Marine Biodiversity*, 50, 1-12.
746 Morgan, S. G., Fisher, J. L., McAfee, S. T., Largier, J. L., & Halle, C. M. (2012). Limited
747 recruitment during relaxation events: larval advection and behavior in an upwelling
748 system. *Limnology and Oceanography*, 57, 457-470.
749 Nanninga, G. B., Saenz-Agudelo, P., Manica, A., & Berumen, M. L. (2014).
750 Environmental gradients predict the genetic population structure of a coral reef fish
751 in the Red Sea. *Molecular Ecology*, 23, 591–602.
752 North, E. W., Gallego, A., & Petitgas, P. (2009). Manual of recommended practices for
753 modelling physical–biological interactions during fish early life. ICES Cooperative
754 Research Report No. 295.
755 Paris, C. B., Helgers, J., Sebille, E., & Srinivasan, A. (2013). Connectivity Modeling
756 System: A probabilistic modeling tool for the multi-scale tracking of biotic and
757 abiotic variability in the ocean. *Environmental Modelling & Software*, 42, 47-54.
758 Parrish, H. R., Nelson, C. S., & Bakun, A. (1981). Transport mechanisms and reproductive
759 success of fishes in the California current. *Biological Oceanography*, 1, 175-203.
760 Priest, M. A., DiBattista, J. D., McIlwain, J. L., Taylor, B. M., Hussey, N. E., & Berumen,
761 M. L. (2016). A bridge too far: dispersal barriers and cryptic speciation in an
762 Arabian Peninsula grouper (*Cephalopholis hemistiktos*). *Journal of Biogeography*,
763 43, 820–832.
764 R Development Core Team. (2008). R: A language and environment for statistical
765 computing. R Foundation for Statistical Computing.
766 Rankin, T. L., & Sponaugle, S. (2011). Temperature influences selective mortality during
767 the early life stages of a coral reef fish. *PloS one*, 6, e16814.
768 Rocha, L. A. (2003). Patterns of distribution and processes of speciation in Brazilian reef
769 fishes. *Journal of Biogeography*, 30, 1161–1171.
770 Saenz-Agudelo, P., DiBattista, J. D., Piatek, M. J., Gaither, M. R., Harrison, H. B.,
771 Nanninga, G. B., & Berumen, M. L. (2015). Seascape genetics along environmental
772 gradients in the Arabian Peninsula: insights from ddRAD sequencing of
773 anemonefishes. *Molecular Ecology*, 24, 6241–6255.
774 Sheppard, C. R. C., & Salm, R. V. (1988). Reef and coral communities of Oman, with a
775 description of a new coral species (Order Scleractinia, genus Acanthastrea).
776 *Journal of Natural History*, 22, 263-279.
777 Shetye, S. R., Gouveia, A. D., & Shenoi, S. C. (1994). Circulation and water masses of the
778 Arabian Sea. *Proceedings of the Indian Academy of Sciences*, 103, 107-123.
779 Smeed, D. A. (2004). Exchange through the Bab el Mandab. *Deep-Sea Research II*, 51,
780 455–474.
781 Stenevik, R. E., Skogen, M., Sundby, S., & Boyer, D. (2003). The effect of vertical and
782 horizontal distribution on retention of sardine (*Sardinops sagax*) larvae in the
783 northern Benguela e observations and modelling. *Fisheries Oceanography*, 12,
784 185e200.
785 Swift, S. A. & Bower, A. S. (2003). Formation and circulation of dense water in the
786 Persian/Arabian Gulf. *Journal of Geophysical Research*, 108, C1, 3004.
787 Thresher, R. E., & Brothers, E. B. (1985). Reproductive ecology and biogeography of Indo-
788 West Pacific angelfishes. *Evolution*. 39: 878-887.

Torquato, F. O., & Muelbert, J. H. (2014). Horizontal and vertical distribution of larvae of *Engraulis anchoita* (Hubbs & Marini 1935) off Albardão, Southern Brazil. *Pan-American Journal of Aquatic Sciences*, 9, 154-166.

Torquato, F. O., Range, P., Ben-Hamadou, R., Sigsgaard, E. E., Thomsen, P. F., Riera, R., … Møller, P. R. (2019). Consequences of marine barriers on genetic diversity of the coral-specialist yellowbar angelfish from the western Indian Ocean. *Ecology and Evolution*, 9, 11215-11226.

Torquato, F., Bouwmeester, J., Range, P., Marshell, A., Priest, M. A., Burt, J. A., ... Ben-Hamadou, R. (2021). Population genetic structure of a major reef-building coral species *Acropora downingi* in northeastern Arabian Peninsula. *Coral Reefs*. doi: 10.1007/s00338-021-02158-y.

Treml, E. A., Roberts, J. J., Chao, Y., Halpin, P. N., Possingham, H. P. & Riginos, C. (2012). Reproductive Output and Duration of the Pelagic Larval Stage Determine Seascape-Wide Connectivity of Marine Populations. *Integrative and Comparative Biology*, 52, 525–537.

Treml, E. A., Roberts, J., Halpin, P. N., Possingham, H. P., & Riginos, C. (2015). The emergent geography of biophysical dispersal barriers across the Indo-West Pacific. *Diversity and Distributions*, 21, 465–476.

UNEP-WCMC, WorldFish Centre, WRI, TNC (2010). Global distribution of warm-water coral reefs, compiled from multiple sources including the Millennium Coral Reef Mapping Project. Version 3.0. Includes contributions from IMaRS-USF and IRD (2005), IMaRS-USF (2005) and Spalding et al. (2001). UN Environment World Conservation Monitoring Centre, Cambridge/UK. URL: http://data.unep-wcmc.org/datasets/1.

van Herwerden, L., McIlwain, J., Al-Oufi, H., Al-Amry, W., & Reyes, A. (2006). Development and application of microsatellite markers for *Scomberomorus commerson* (Perciformes; Teleostei) to a population genetic study of Arabian Peninsula stocks. *Fisheries Research*, 79, 258-266.

Vaughan, G. O., Al-Mansoori, N., & Burt, J. A . (2019) The Arabian Gulf. In C. Sheppard (Ed), *World seas: An environmental evaluation* (pp 1–23). Massachuetts: Academic Press.

Yao, F., & Johns, W. E. (2010). A HYCOM modeling study of the Persian Gulf: 2. Formation and export of Persian Gulf Water. *Journal of Geophysical Research: Oceans*, 115(C11).

Zuur, A. F., Ieno, E. N., & Elphick, C. S. (2010). A protocol for data exploration to avoid common statistical problems. *Methods in Ecology and Evolution*, 1, 3-14.

BIOSKETCH

Felipe Torquato is interested in the origin and distribution of biodiversity at all ecological levels. This work represents a component of his PhD work at the Natural History Museum of Denmark under the supervision of Peter R. Møller.

Author contributions: F. T. and P. R. M. conceived the idea; F. T. designed and ran the biophysical models, and led the writing with assistance from P. R. M.

TABLES

TABLE 1. Range in biological parameter values to characterize the 72 hypothetical model taxa.

PLD (days)	Spawning periodicity	Larval mortality	Vertical migration	Reproductive output
20	Annual	High	Yes	High
30	Summer	Low	No	Low
40	Winter			

FIGURES

Legends

FIGURE 1. Study region. Northwestern Indian Ocean with previously described barriers depicted as shaded line. (a) Bab-el-Mandeb Strait, (b) Upwelling off Oman and (c) Strait of Hormuz.

FIGURE 2. Results of the simulation study showing the effects of the biological traits on the permeability of the Bab-el-Mandeb Strait in both directions (in and out). The red triangles represent the mean value. Diverging letters above boxplots indicate significant differences according to Tukey's post-hoc analysis, with capital and lowercase letters distinguishing the permeability direction.

FIGURE 3. Results of the simulation study showing the effects of the biological traits on the permeability of the Strait of Hormuz in both directions (in and out). The red triangles represent the mean value. Diverging letters above boxplots indicate significant differences according to Tukey's post-hoc analysis, with capital and lowercase letters distinguishing the permeability direction.

FIGURE 4. Results of the simulation study showing the effects of the biological traits on local retention along the Omani coast. Diverging letters above boxplots indicate significant differences according to Tukey's post-hoc analysis.

FIGURE 5. Modeled dispersal paths of epipelagic virtual larvae with larval duration of 40 days released in the wintertime from (a) the Red Sea, (b) Gulf of Aden, (c) Arabian Sea, (d) Sea of Oman and (e) Arabian/Persian Gulf. For sake of visualization, one larva was released from each habitat cell (total of 181, represented by the red dots) per day in 2019. The distances travelled by the larvae are represented in (f).

FIGURE 6. Modeled dispersal paths of epipelagic virtual larvae with larval duration of 40 days released in the summertime from (a) the Red Sea, (b) Gulf of Aden, (c) Arabian Sea, (d) Sea of Oman and (e) Arabian/Persian Gulf. For sake of visualization, one larva was released from each habitat cell (total of 181, represented by the red dots) per day in 2019. The distances travelled by the larvae are represented in (f).

FIGURE 1.

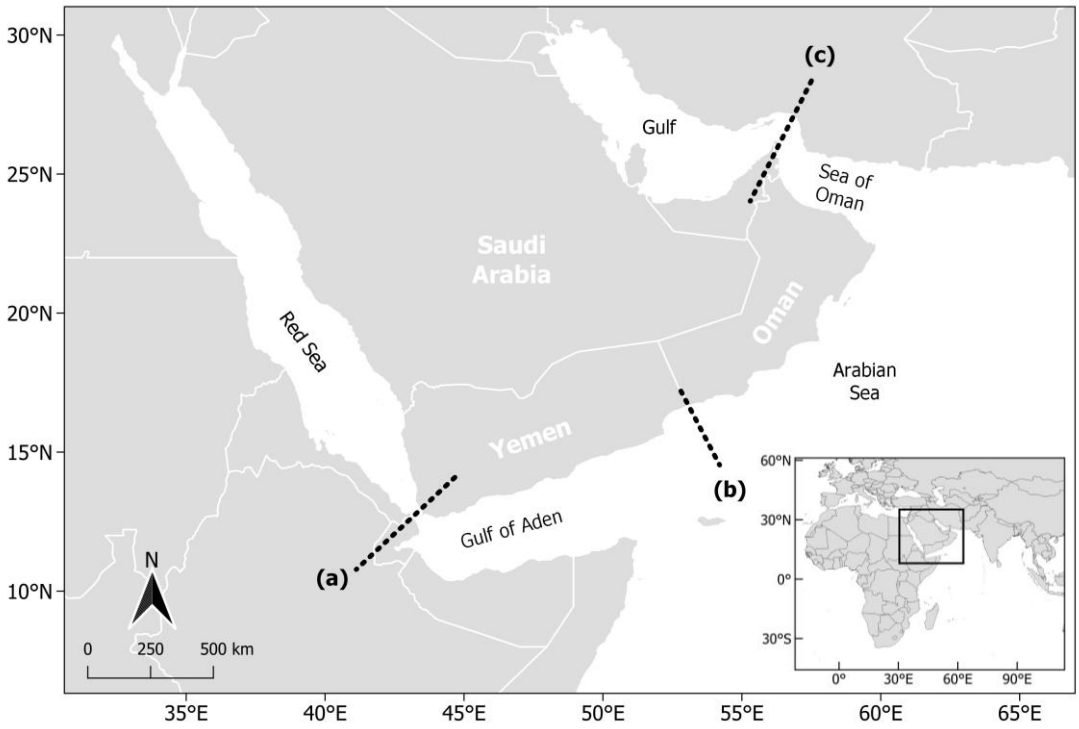

FIGURE 2.

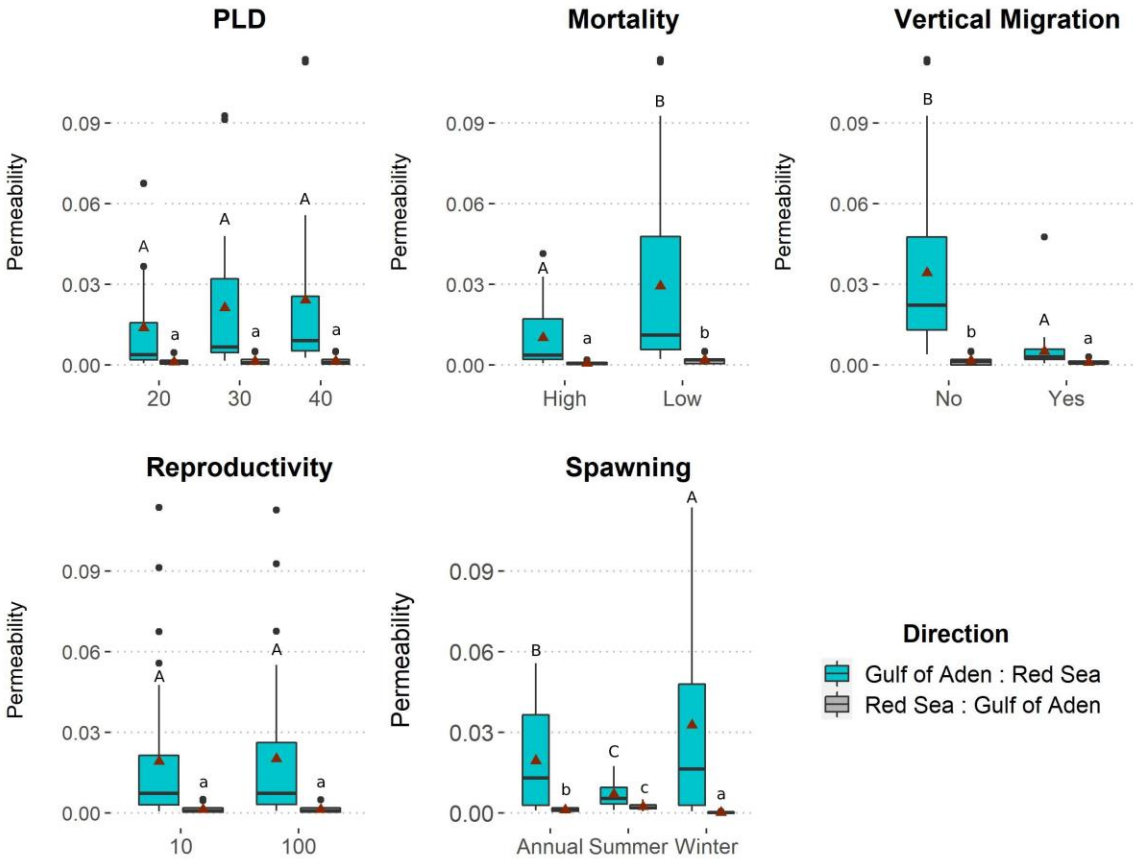
PLD
Mortality
Vertical Migration
Reproductivity
Spawning
Permeability
0.09
0.06
0.03
0.00
20
30
40
High
Low
No
Yes
10
100
Annual
Summer
Winter
Direction
Gulf of Aden : Red Sea
Red Sea : Gulf of Aden

FIGURE 3.

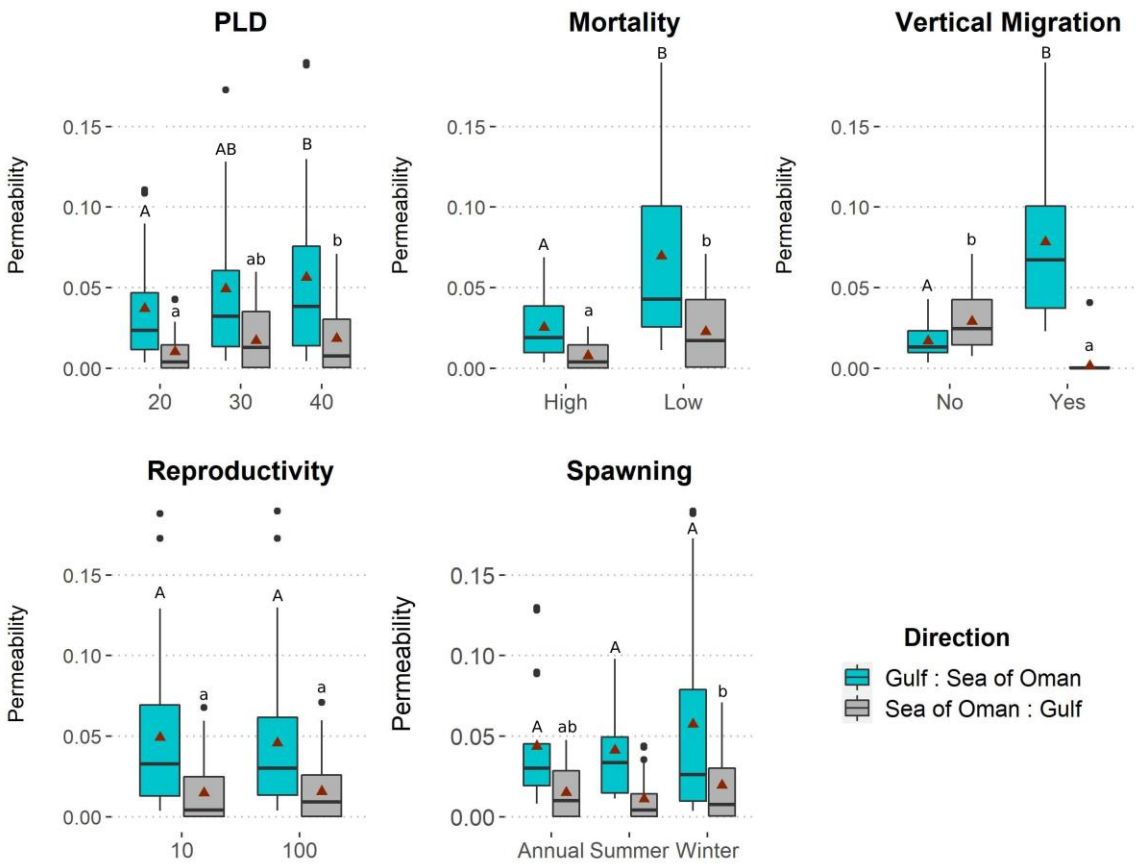
PLD
Mortality
Vertical Migration
Reproductivity
Spawning
Permeability
0.15
0.10
0.05
0.00
A
a
AB
ab
B
b
20
30
40
High
Low
No
Yes
10
100
Annual
Summer
Winter
Direction
Gulf : Sea of Oman
Sea of Oman : Gulf

FIGURE 4.

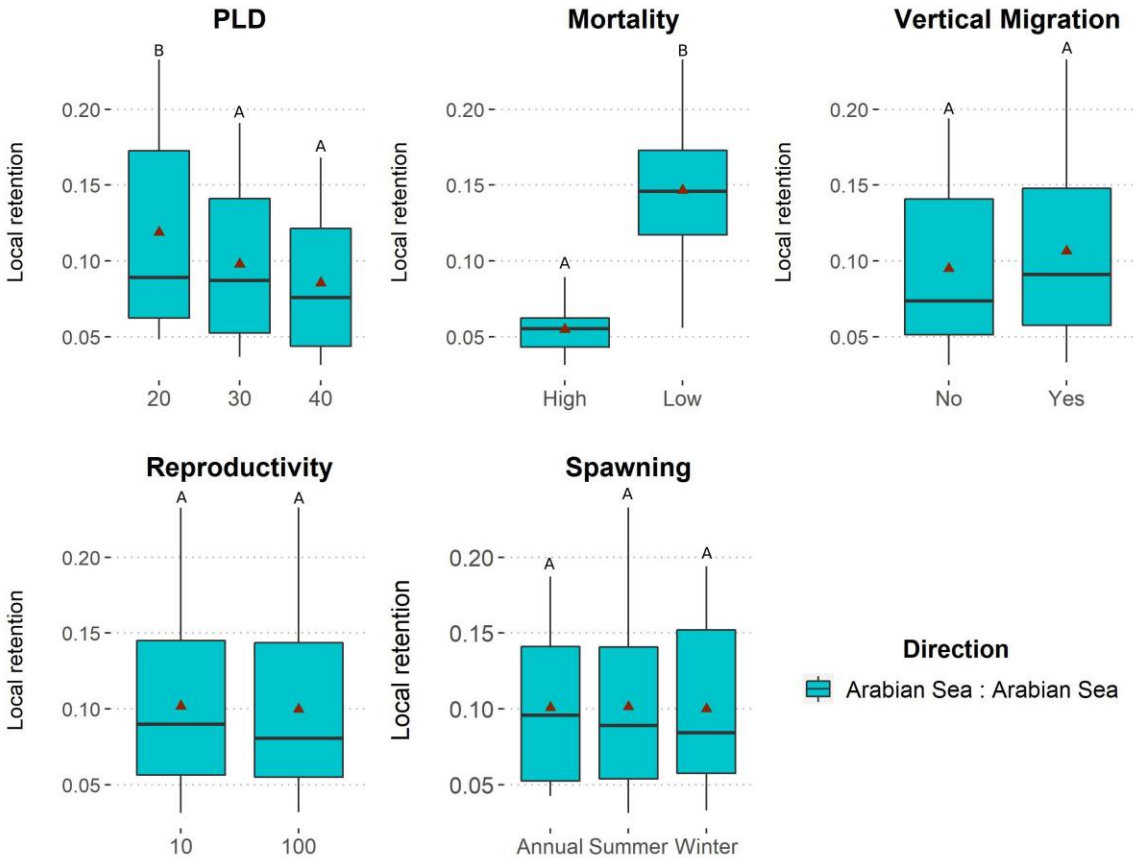
PLD
Mortality
Vertical Migration
Reproductivity
Spawning
Local retention
0.20
0.15
0.10
0.05
B
A
A
20
30
40
High
Low
No
Yes
10
100
Annual
Summer
Winter
Direction
Arabian Sea : Arabian Sea

FIGURE 5.

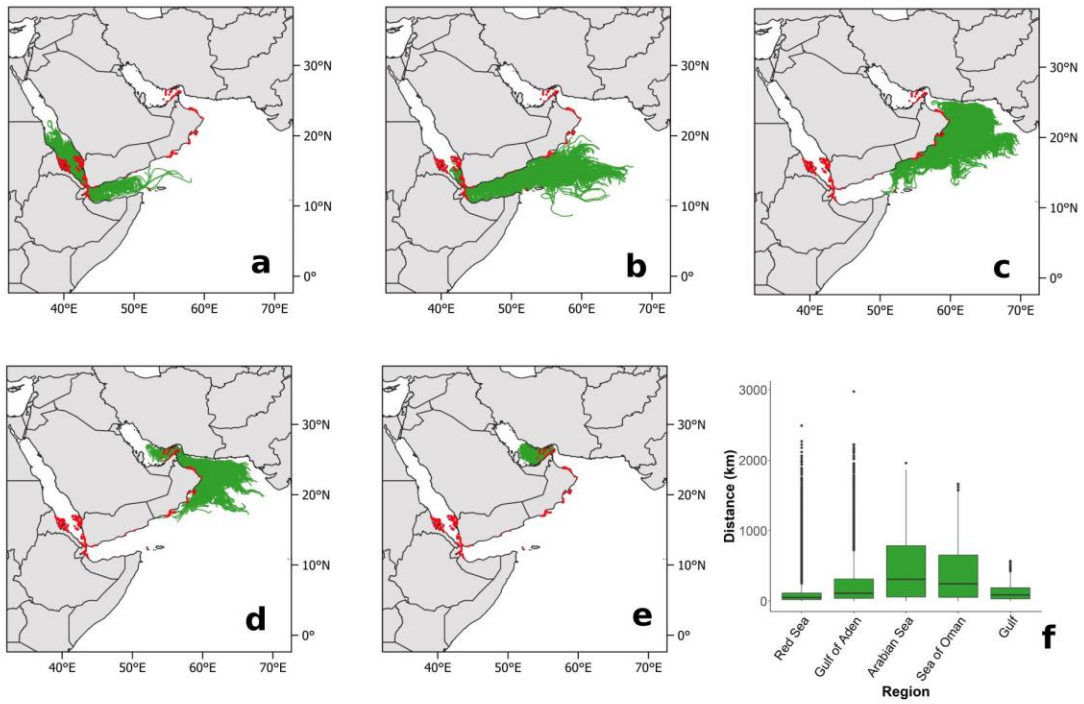

988
989
990 **FIGURE 6.**

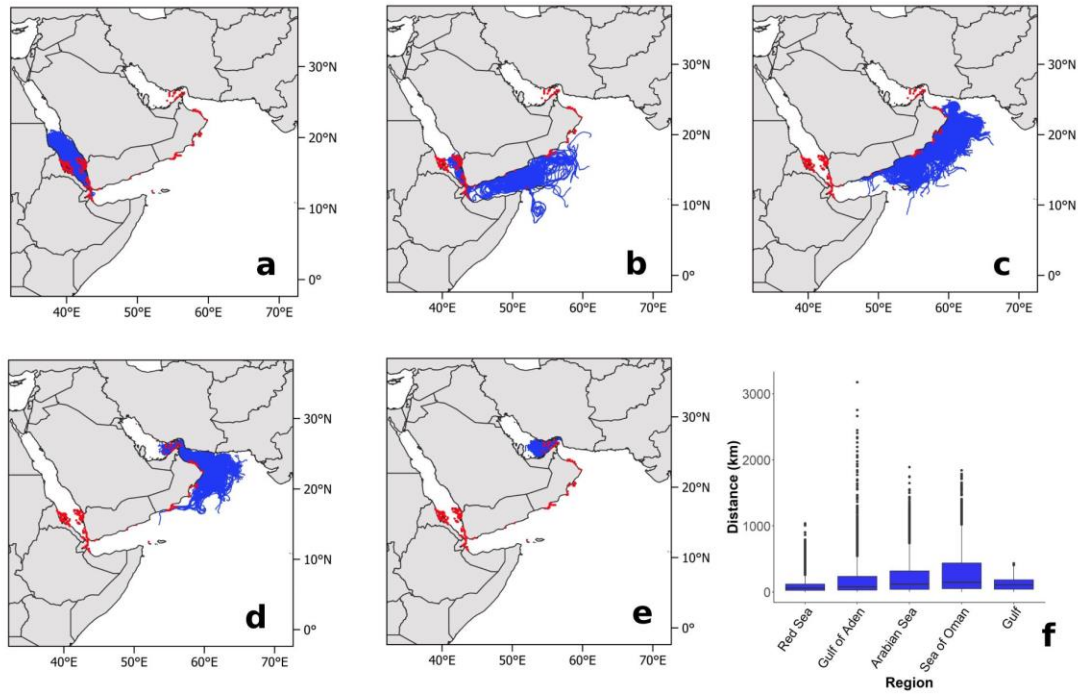

991
992
993

Journal of Biogeography

SUPPORTING INFORMATION

Felipe Torquato & Peter R. Møller

Appendix S1. Visualization of hydrodynamic model, GIS-based seascape module and idealized vertical migration.

FIGURES

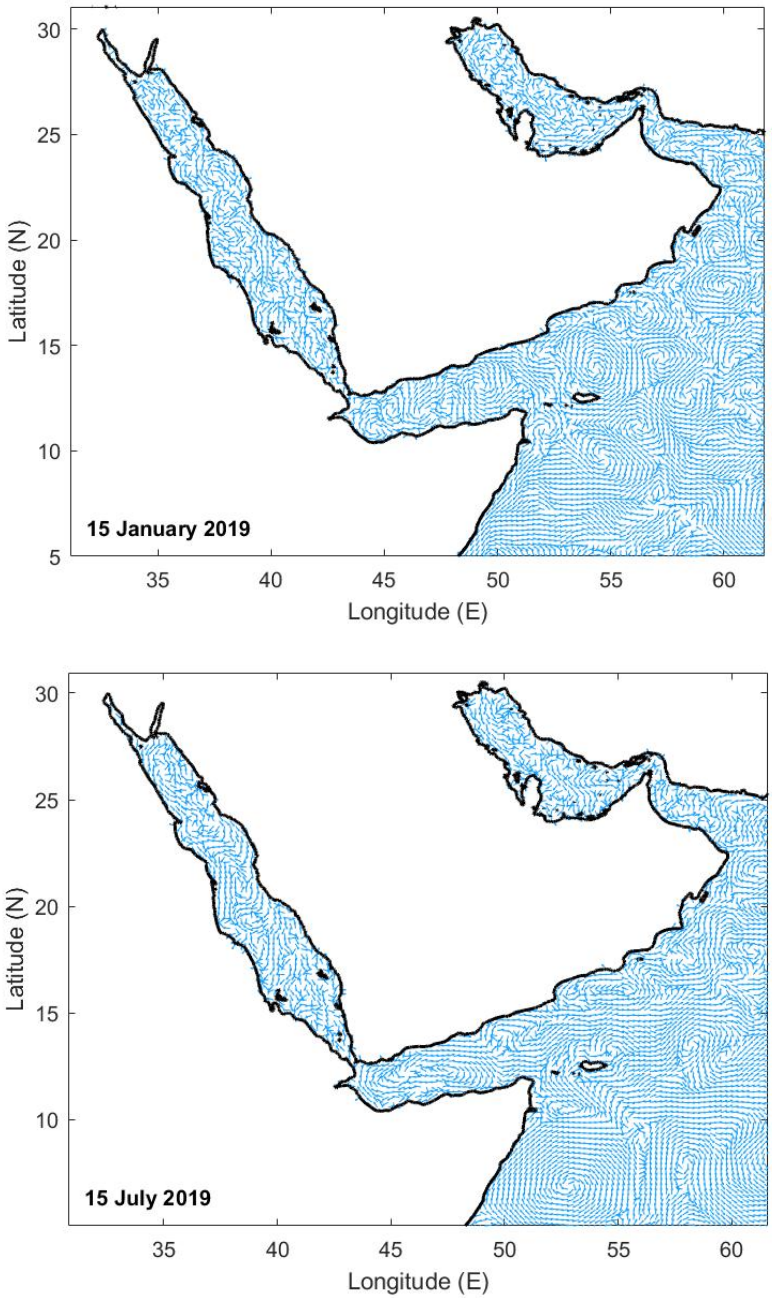

Fig. S1.1. Ocean circulation around the Arabian Peninsula in January 2019 and July 2019.

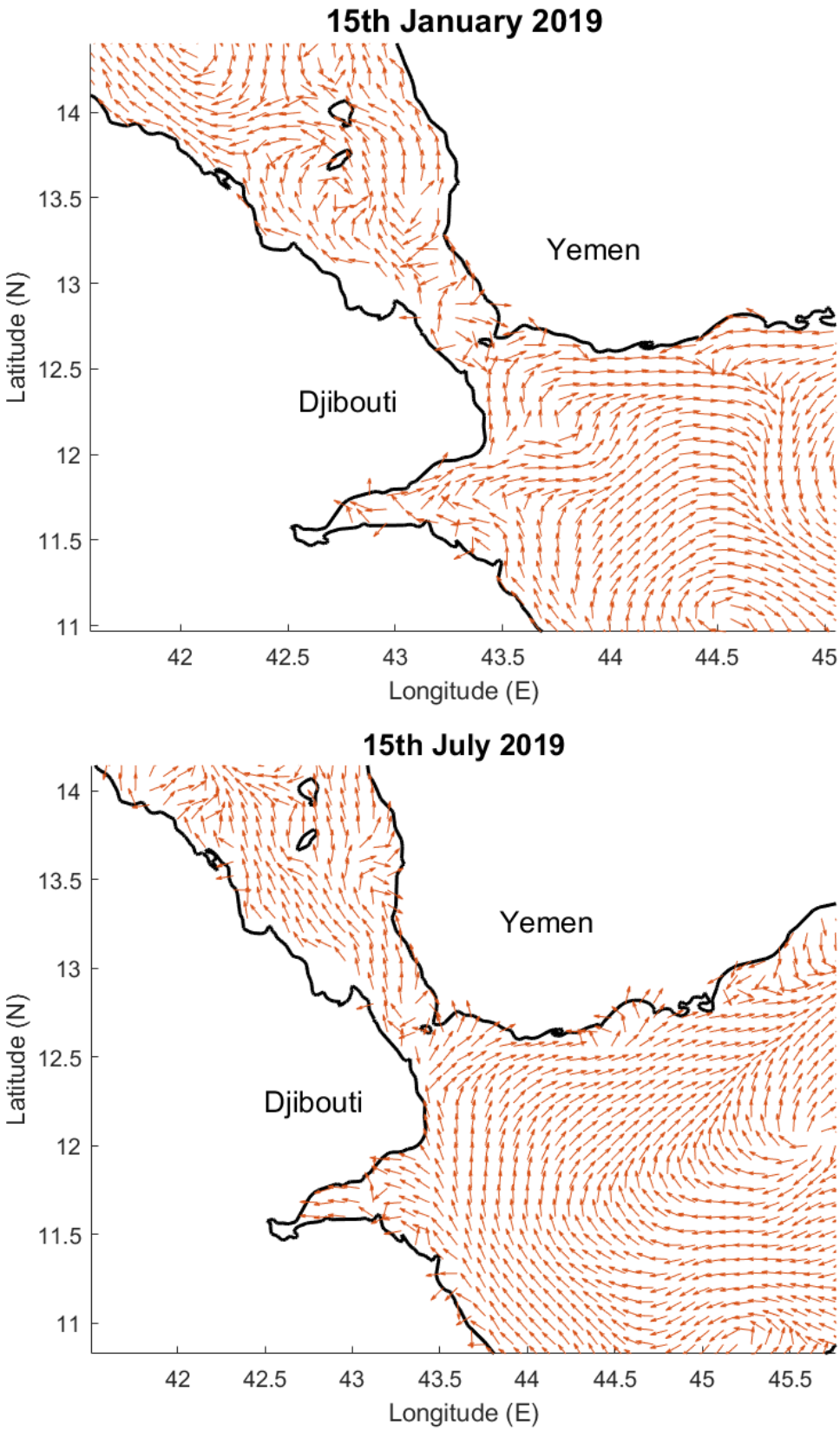

Fig. S1.2. Ocean circulation across the Bab-el-Mandeb strait (between the Red Sea and the Gulf of Aden) in January 2019 and July 2019.

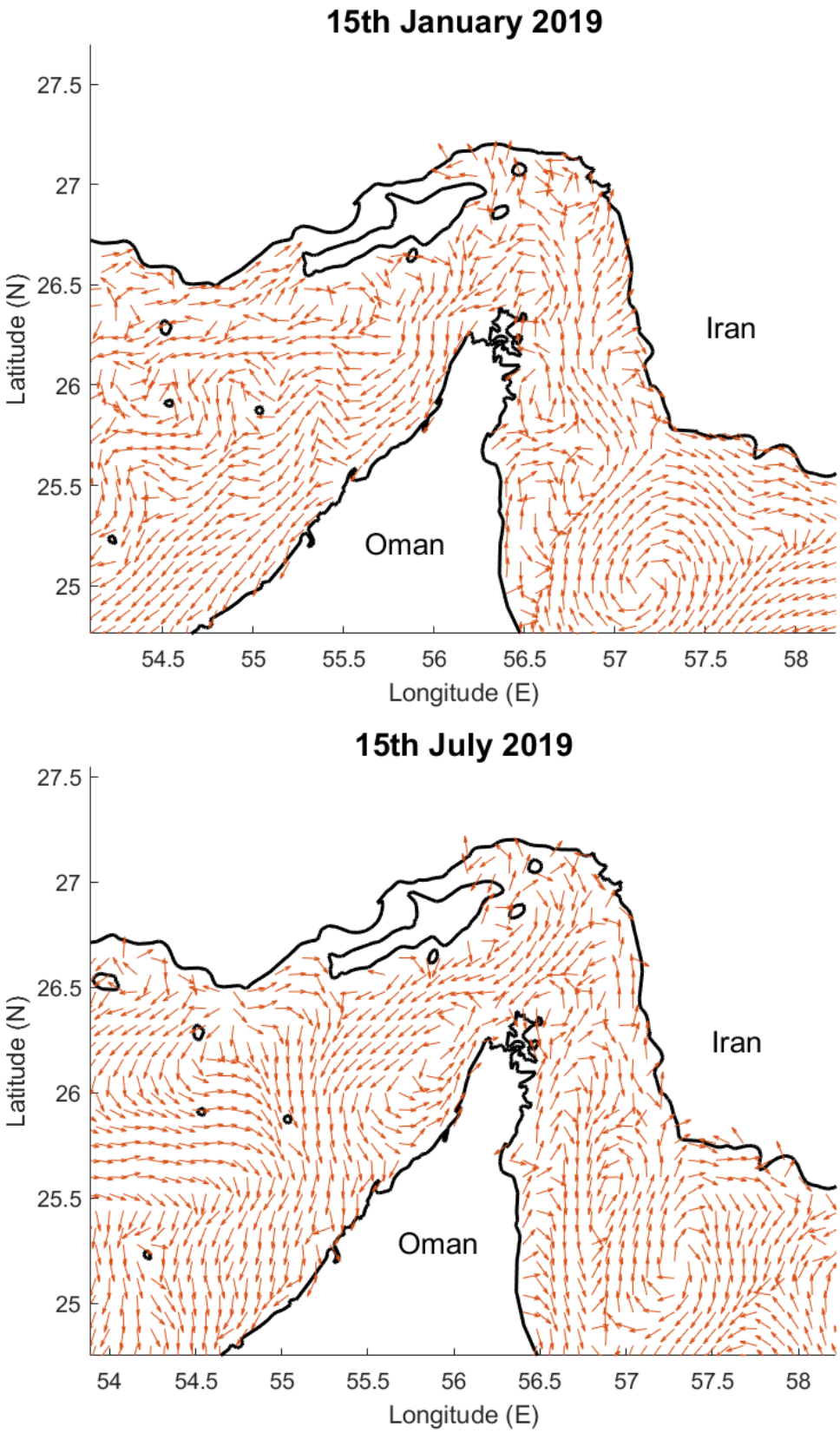

Fig. S1.3. Ocean circulation across the Strait of Hormuz (between the Arabian/Persian Gulf and the Sea of Oman) in January 2019 and July 2019.

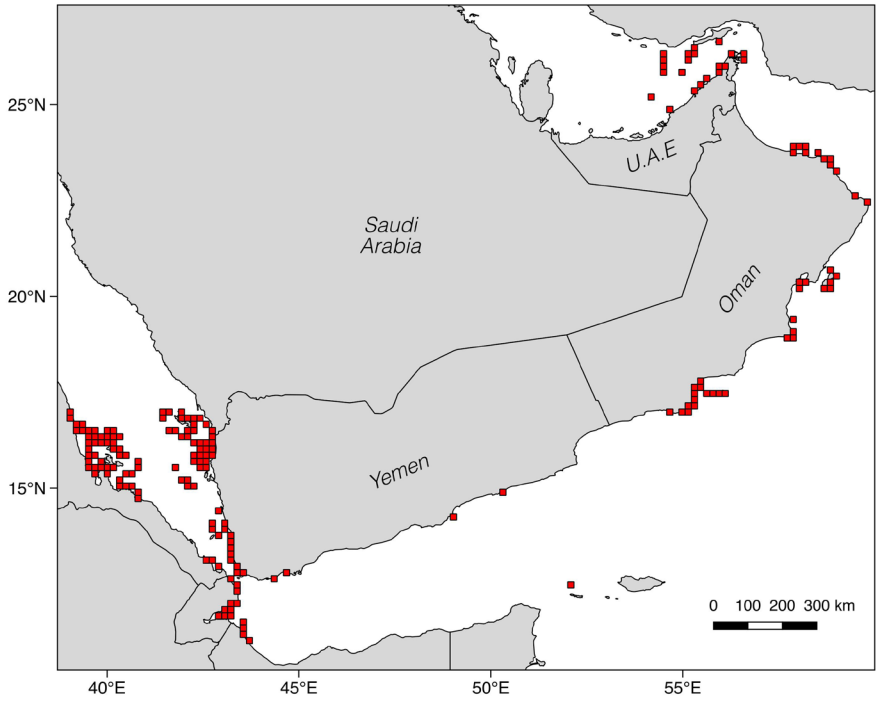

Fig. S1.4. The 181 polygons (in red) representing the sites of releasing and settlement along the Arabian Peninsula.

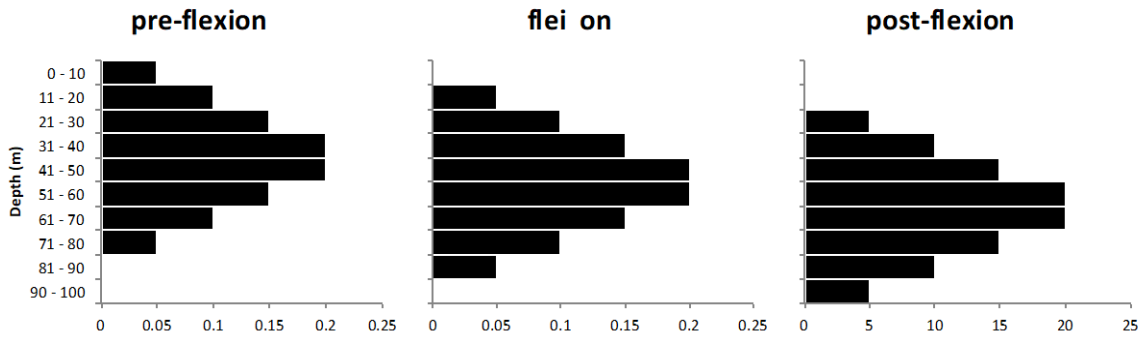

Fig. S1.5. Idealized vertical distribution of fish larvae at three ontogenetic stages: pre-flexion, flexion and post-flexion.

Appendix S2. Assessing model saturation

Methods

Sensitivity analyses of some parameters can potentially improve the accuracy of the model (North et al., 2009). Here, the releasing frequency was computed to saturate all possibilities of dispersal based on the connectivity matrix. To determine the release frequency, we conducted a numerical experiment over five months in 2019 (January, March, June, September and December). In this experiment particles were release from the 181 polygons, and the number of released particles remained constant (one hundred) while the releasing frequency varied from 3 hours (baseline) to 24 hours (6 h, 12 h and 24 h).

All values were extracted from the average matrix, vectored and used to calculate the fraction of unexplained variance (FUV) (Simons et al., 2013). To do so, the simulation that released 100 particles/3h over the five months was used as the baseline and compared to their peers in a linear model. The coefficient of determination (r^2) was then calculated between each baseline/increment pairing. A 0.05 threshold FUV variance was used to define the point where variance in FUV was minimal (Ross et al., 2016; Simons et al., 2013).

The same experiment was conducted to determine the value of horizontal diffusion by comparing three values, namely: 5 $m.s^{-1}$, 50 $m.s^{-1}$ and 100 $m.s^{-1}$.

Results

Release frequency showed no significant differences whether 100 particles were released every 3 or 24 hours. The second experiment, in turn showed that 50

$m.s^{-1}$ was significantly different compared to 5 $m.s^{-1}$, but not different compared to 100 $m.s^{-1}$.

Release Frequency

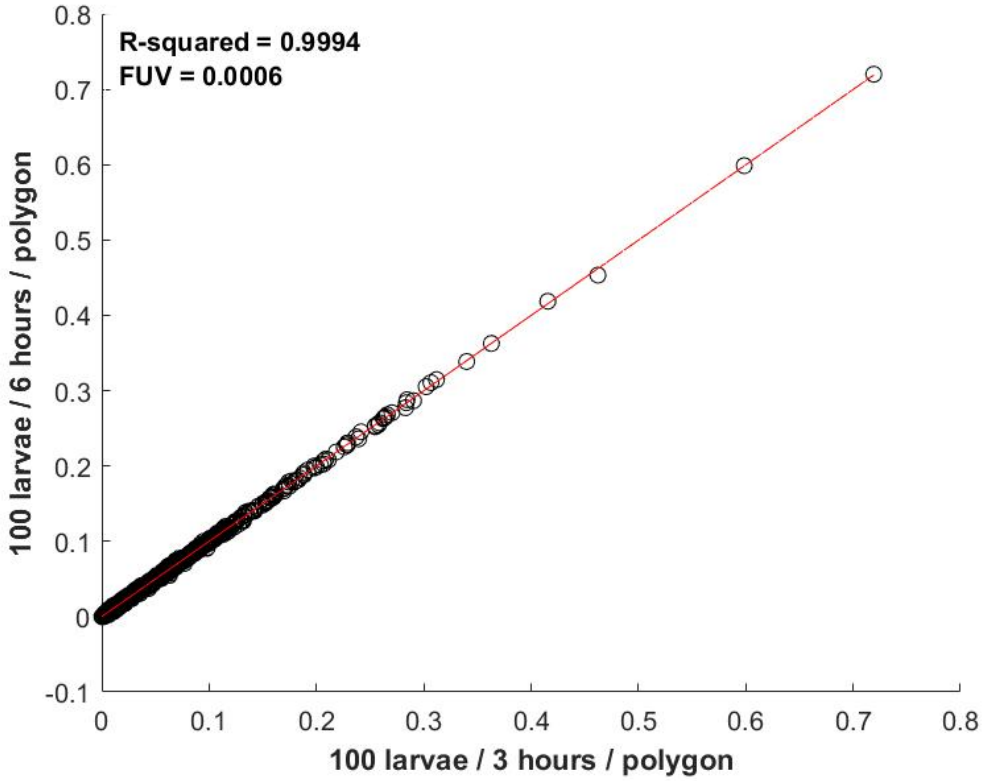

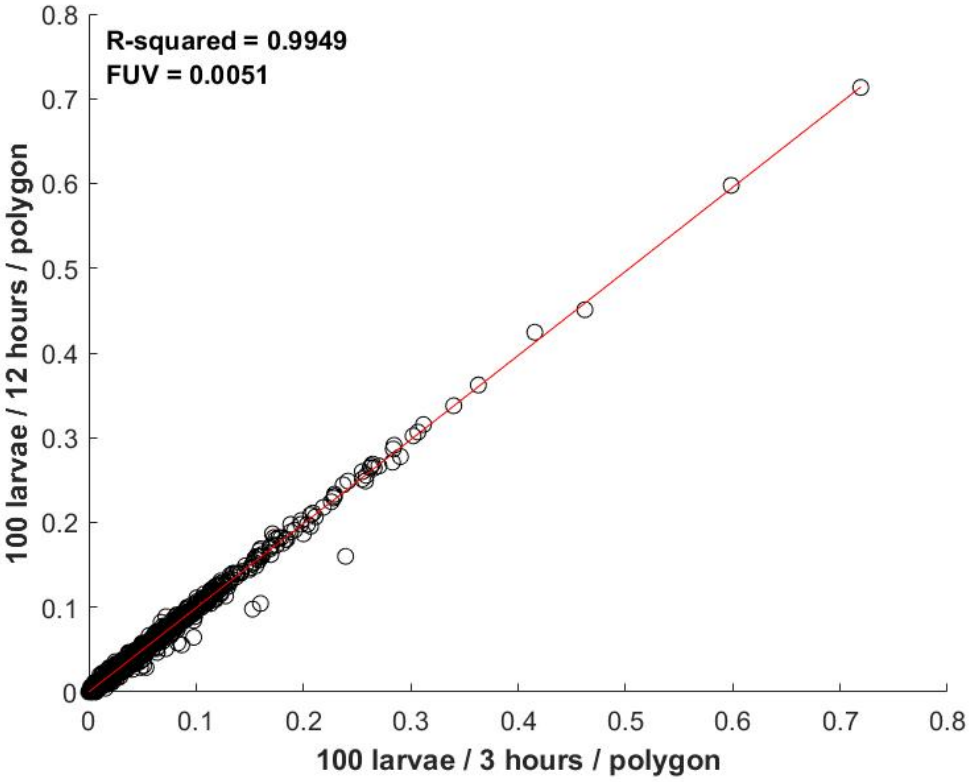
R-squared = 0.9949
FUV = 0.0051
100 larvae / 12 hours / polygon
100 larvae / 3 hours / polygon
0
0.1
0.2
0.3
0.4
0.5
0.6
0.7
0.8

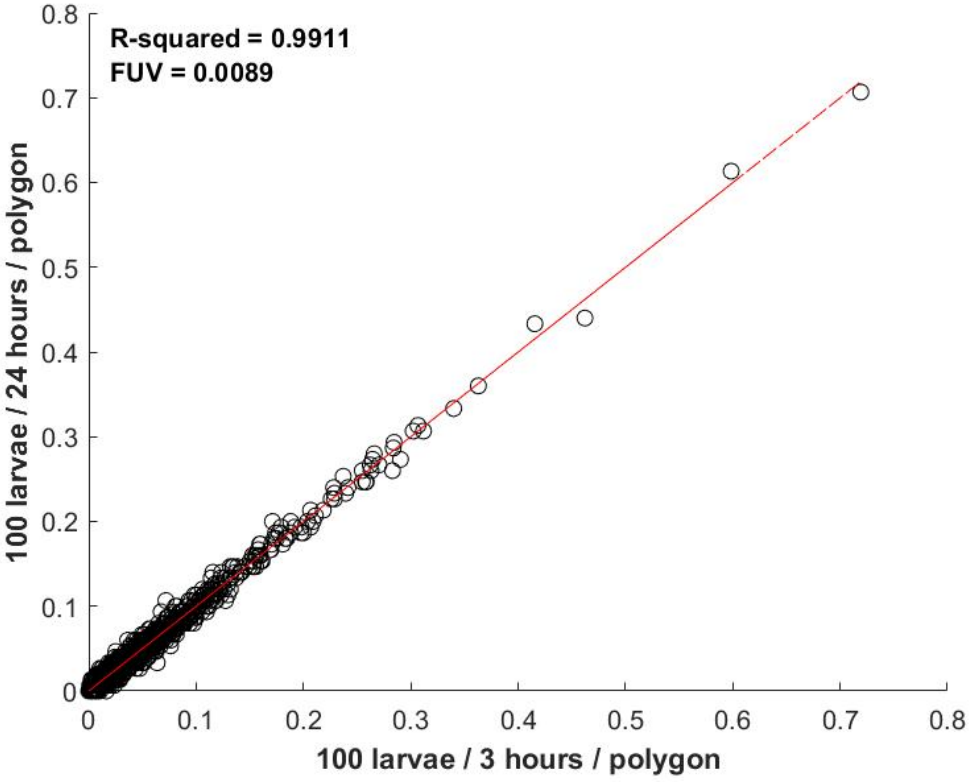
R-squared = 0.9911
FUV = 0.0089
100 larvae / 24 hours / polygon
100 larvae / 3 hours / polygon
0
0.1
0.2
0.3
0.4
0.5
0.6
0.7
0.8

Horizontal Diffusion

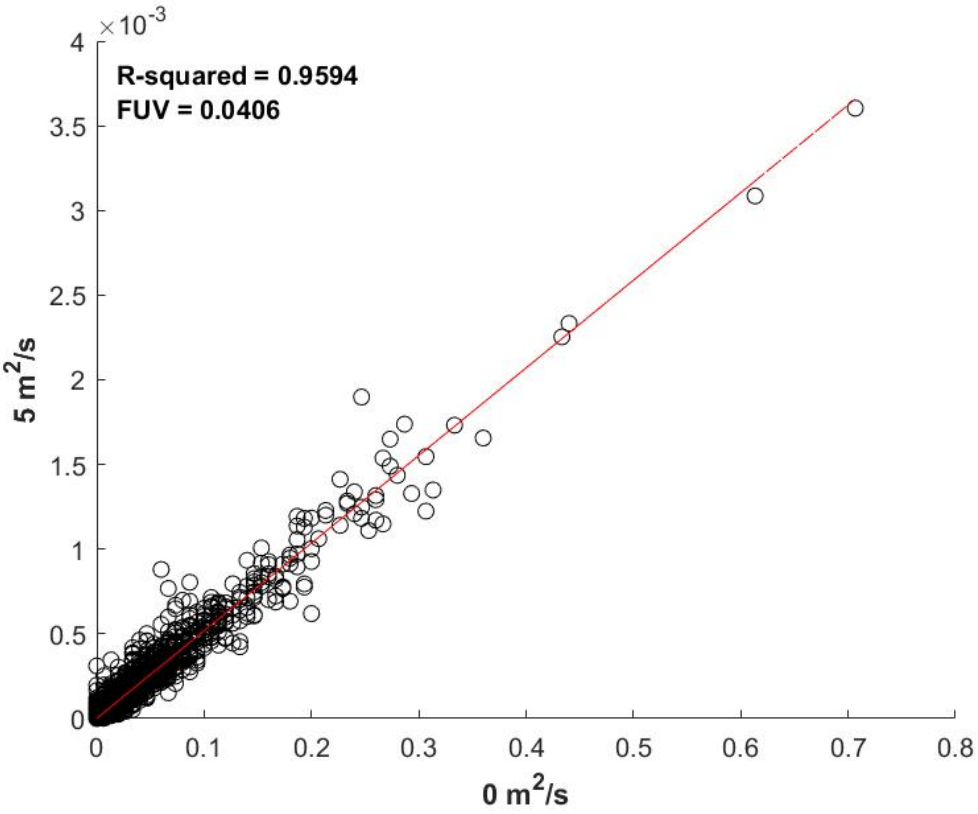

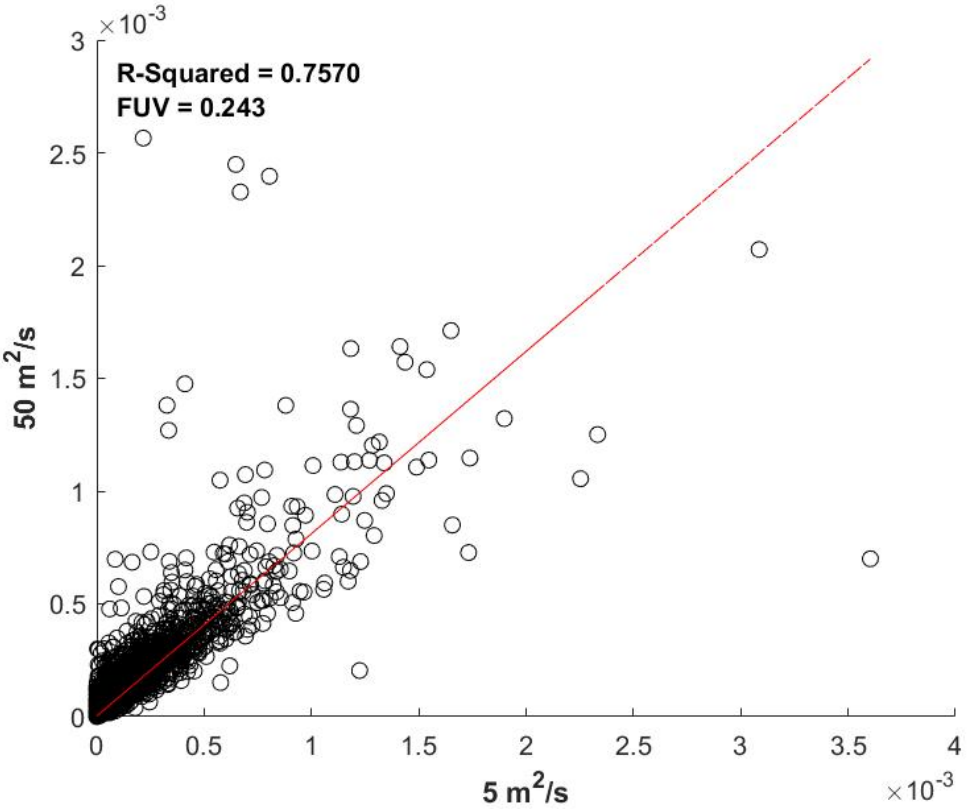

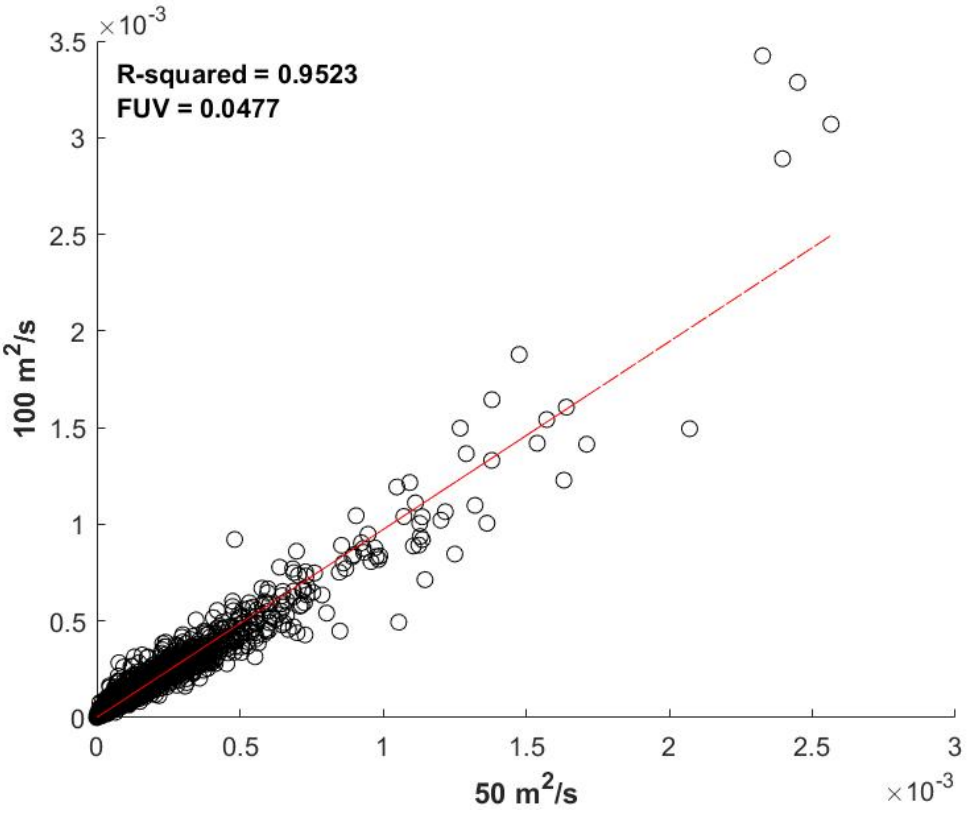
×10-3
3.5
3
2.5
2
1.5
1
0.5
0
R-squared = 0.9523
FUV = 0.0477
100 m2/s
0
0.5
1
1.5
2
2.5
3
50 m2/s
×10-3

Appendix S3. Results

TABLES

Table S3.1. Summary statistics of the tested beta regression models, where (*) highlights significant explanatory variables at a level of 5% of significance.

	Estimate	Std. Error	z-value	p-value	R-squared
Bab-el-Mandeb Strait (Red Sea : Gulf of Aden)					
Intercept	-7.2269011	0.1128531	-64.038	< 2e-16 ***	0.7316
PLD: 30	0.2411450	0.089063	2.708	0.00678 **	
PLD: 40	0.2862904	0.0882429	3.244	0.00118 **	
Mortality: low	0.9075848	0.0772678	11.746	< 2e-16 ***	
Vertical migration	-0.4222897	0.0718519	-5.877	4.17e-09 ***	
Spawning: winter	-2.1813041	0.0765547	-12.652	< 2e-16 ***	
Spawning: summer	0.6981031	0.1724094	9.119	< 2e-16 ***	
Producitivity: high	-0.0006879	0.0007823	-0.879	0.3792	
Bab-el-Mandeb Strait (Gulf of Aden : Red Sea)					
Intercept	-4.3080607	0.1238068	-34.797	< 2e-16 ***	0.7868
PLD: 30	0.3973543	0.1012779	3.923	8.73e-05 ***	
PLD: 40	0.5788425	0.0983284	5.887	3.94e-09 ***	
Mortality: low	1.0002121	0.0847535	11.801	< 2e-16 ***	
Vertical migration	-2.1100997	0.1145143	-18.427	< 2e-16 ***	
Spawning: winter	0.5609861	0.0855140	6.56	5.37e-11 ***	
Spawning: summer	-1.0141382	0.1238914	-8.186	2.71e-16 ***	
Producitivity: high	0.0000449	0.0008555	0.052	0.958	

Table S3.2. Summary statistics of the tested beta regression models, where (*) highlights significant explanatory variables at a level of 5% of significance.

Strait of Hormuz (Arabian Gulf : Gulf of Oman)					
	Estimate	**Std. Error**	**z-value**	**p-value**	**R-squared**
Intercept	-4.9124546	0.1505193	-32.637	< 2e-16 ***	0.8111
PLD: 30	0.2364959	0.1036752	2.281	0.02254 *	
PLD: 40	0.4163682	0.1006201	4.138	3.5e-05 ***	
Mortality: low	0.9828239	0.0878447	11.188	< 2e-16 ***	
Vertical migration	1.6024823	0.1009071	15.881	< 2e-16 ***	
Spawning: winter	0.2730849	0.0973578	2.805	0.00503 **	
Spawning: summer	-0.042459	0.103221	-0.411	0.68082	
Producitivity: high	-0.0011347	0.0008993	-1.262	0.20704	
Strait of Hormuz (Gulf of Oman : Arabian Gulf)					
Intercept	-4.5225190	0.1126374	-40.151	< 2e-16 ***	0.9409
PLD: 30	0.4369342	0.0918442	4.757	1.96e-06 ***	
PLD: 40	0.5859257	0.0896038	6.539	6.19e-11 ***	
Mortality: low	0.9839256	0.0767302	12.823	< 2e-16 ***	
Vertical migration	-3.2631946	0.1573465	-20.739	< 2e-16 ***	
Spawning: winter	0.3496437	0.0819124	4.269	1.97e-05 ***	
Spawning: summer	-0.2114086	0.0922269	-2.292	0.0219 *	
Producitivity: high	-0.0001485	0.0007732	-0.192	0.8476	

Table S3.3. Summary statistics of the tested beta regression models, where (*) highlights significant explanatory variables at a level of 5% of significance.

Upwelling off Oman (Arabian Sea : Arabian Sea)					
	Estimate	**Std. Error**	**z-value**	**p-value**	**R-squared**
Intercept	-2.6539714	0.099316	-26.722	< 2e-16 ***	0.8092
PLD: 30	-0.2057318	0.0772098	-2.665	0.00771 **	
PLD: 40	-0.3572552	0.0796759	-4.484	7.33e-06 ***	
Mortality: low	1.0406014	0.0703126	14.800	< 2e-16 ***	
Vertical migration	0.1369907	0.0648438	2.113	0.03463 *	
Spawning: winter	-0.0412799	0.0791164	-0.522	0.60184	
Spawning: summer	-0.0419393	0.0791261	-0.530	0.59609	
Producitivity: high	-0.0004301	0.0007196	-0.598	0.55002	

FIGURES

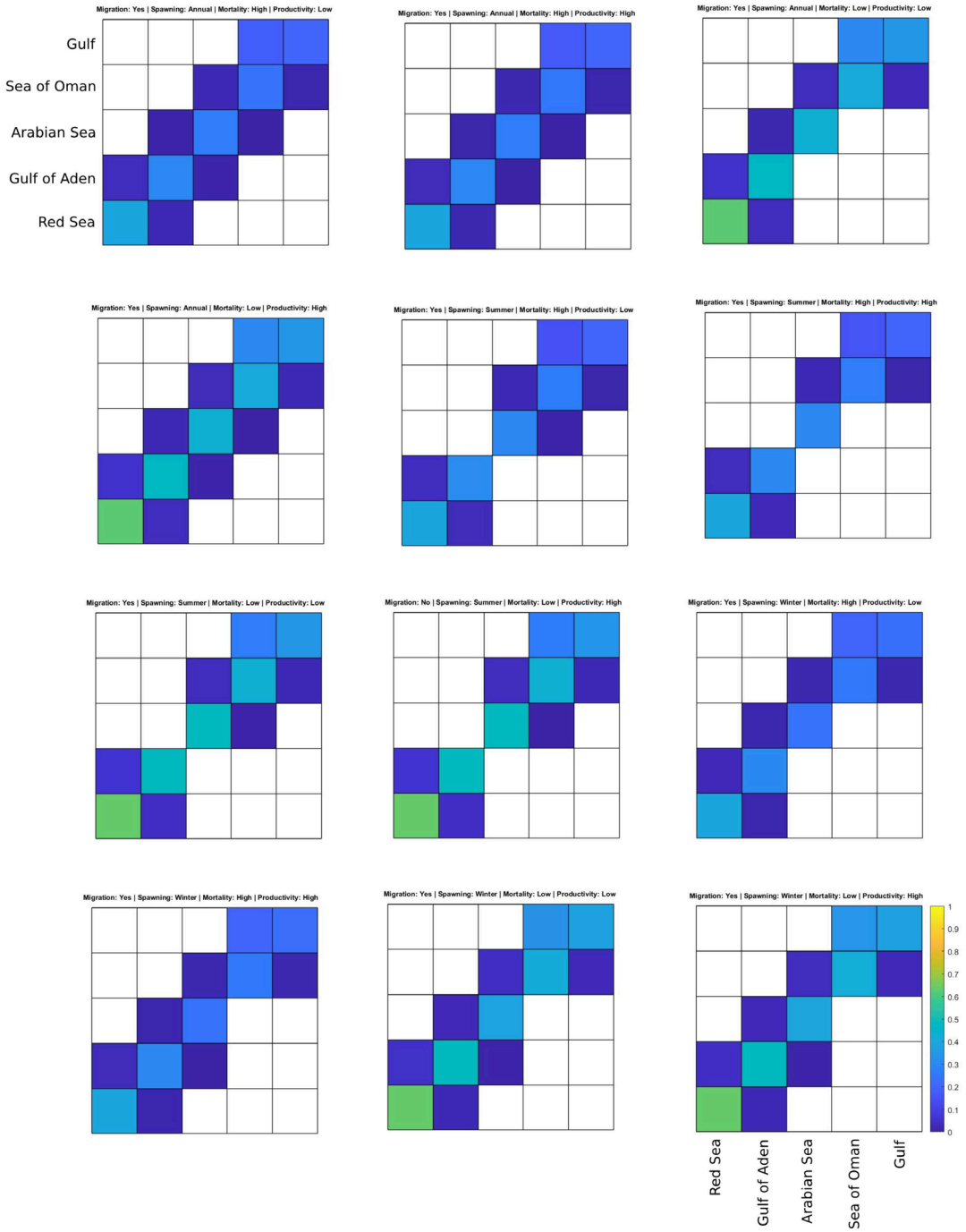

Fig. S3.1. Potential connectivity matrix with larval duration of 20 days. The colorbar shows the root square of the proportion of survived larvae exchanged between each release (y-axis) and settlement (x-axis) region.

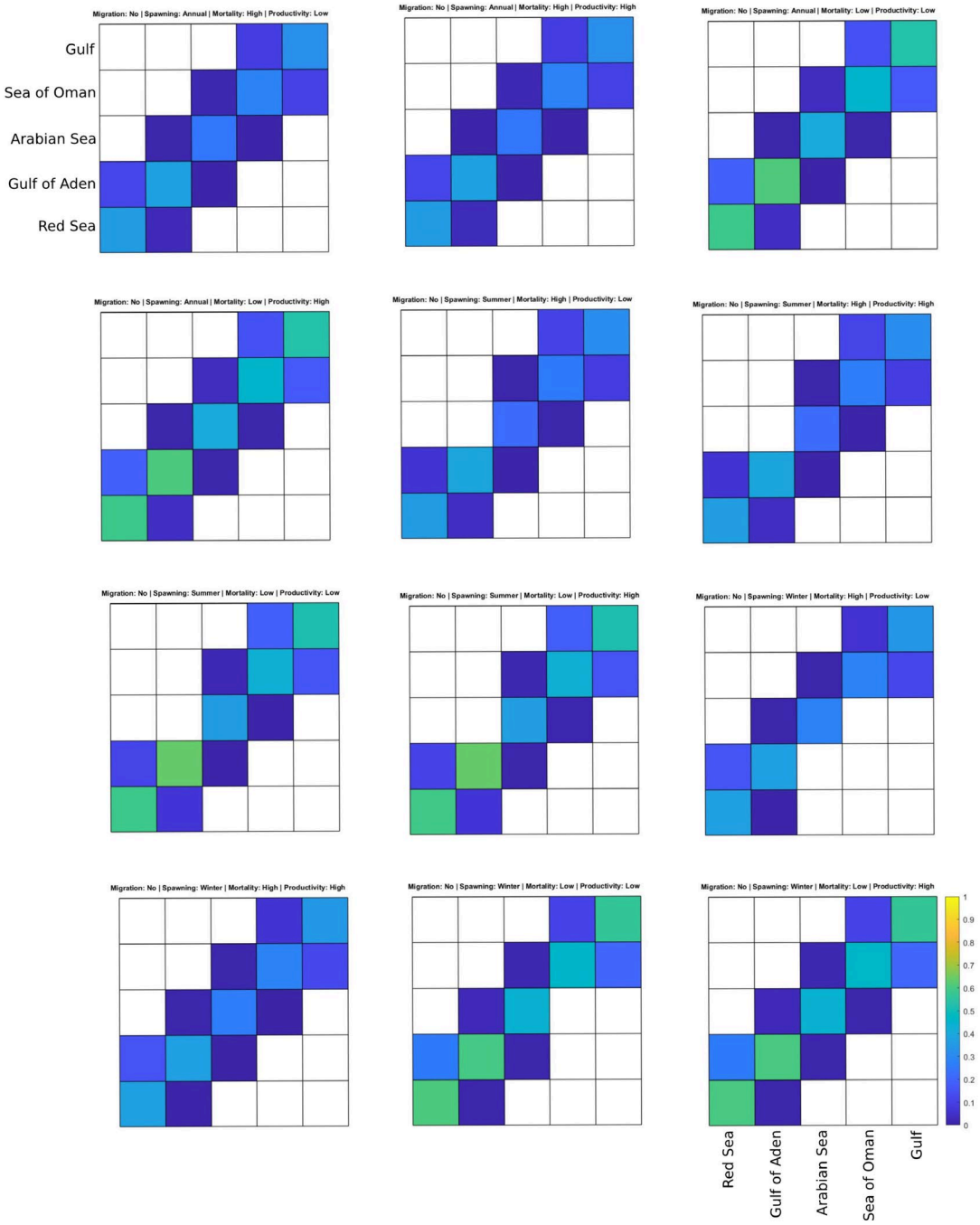

Fig. S3.1 cont. Potential connectivity matrix with larval duration of 20 days. The colorbar shows the root square of the proportion of survived larvae exchanged between each release (y-axis) and settlement (x-axis) region.

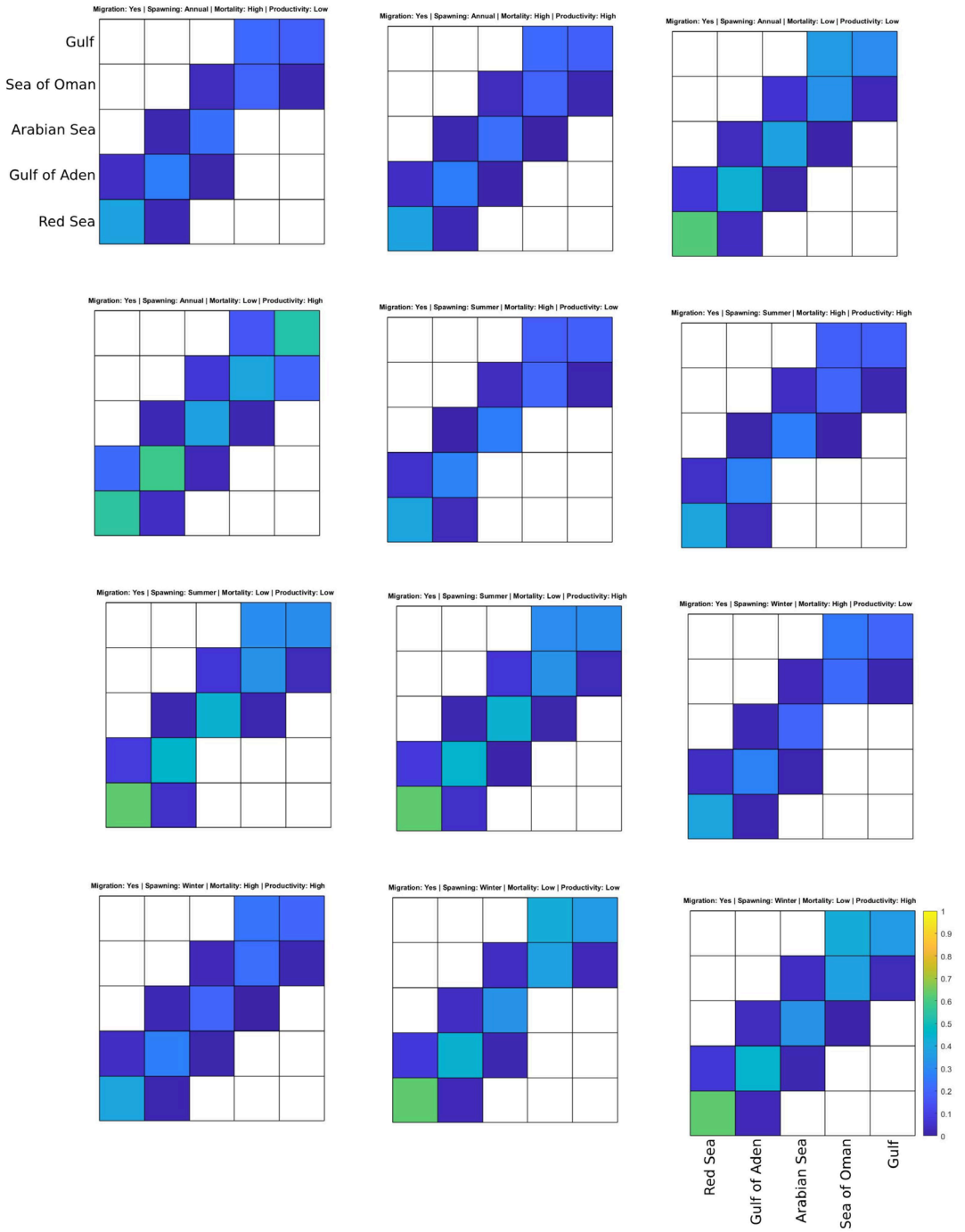

Fig. S3.2. Potential connectivity matrix with larval duration of 30 days. The colorbar shows the root square of the proportion of survived larvae exchanged between each release (y-axis) and settlement (x-axis) region.

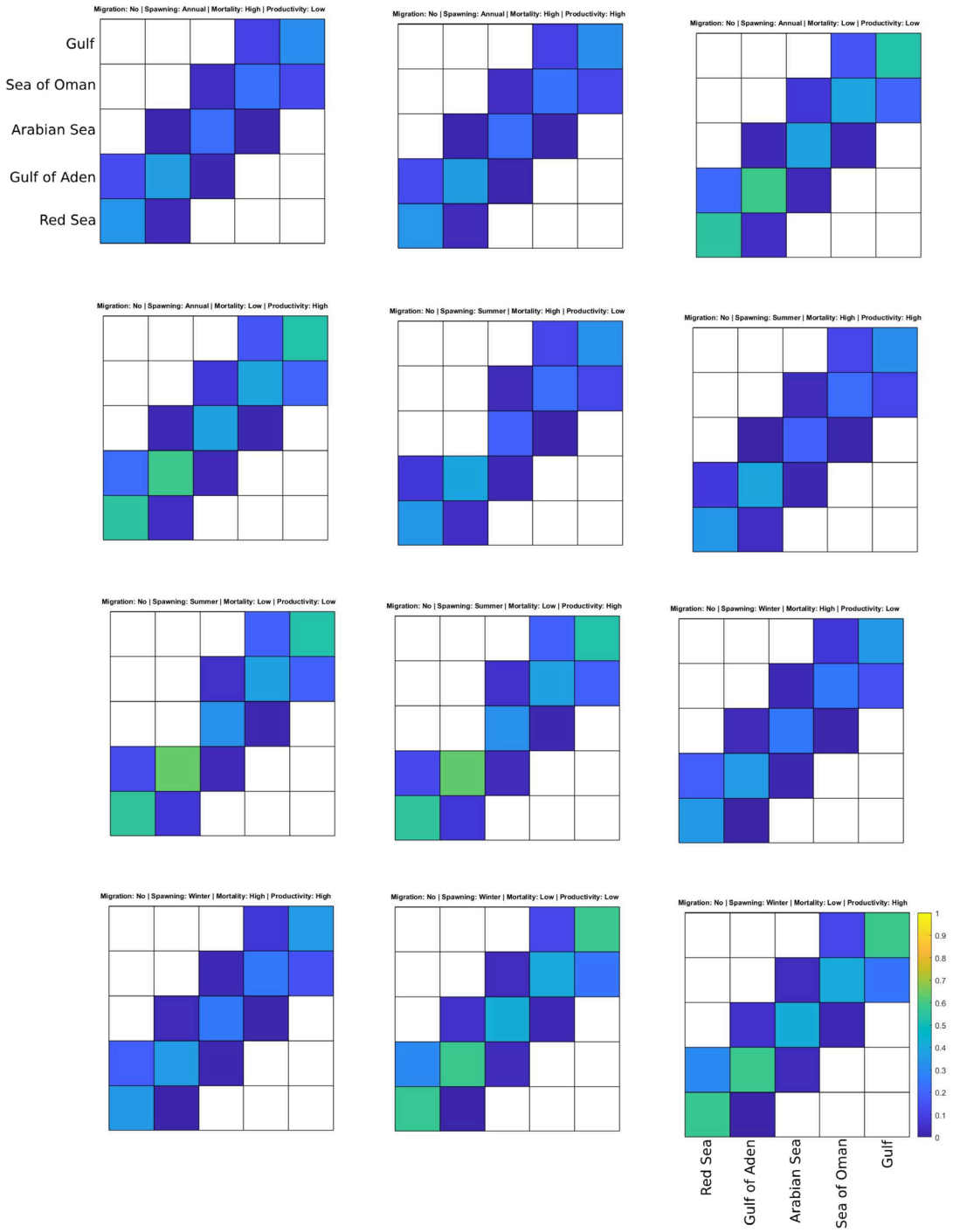

Fig. S3.2 cont. Potential connectivity matrix with larval duration of 30 days. The colorbar shows the root square of the proportion of survived larvae exchanged between each release (y-axis) and settlement (x-axis) region.

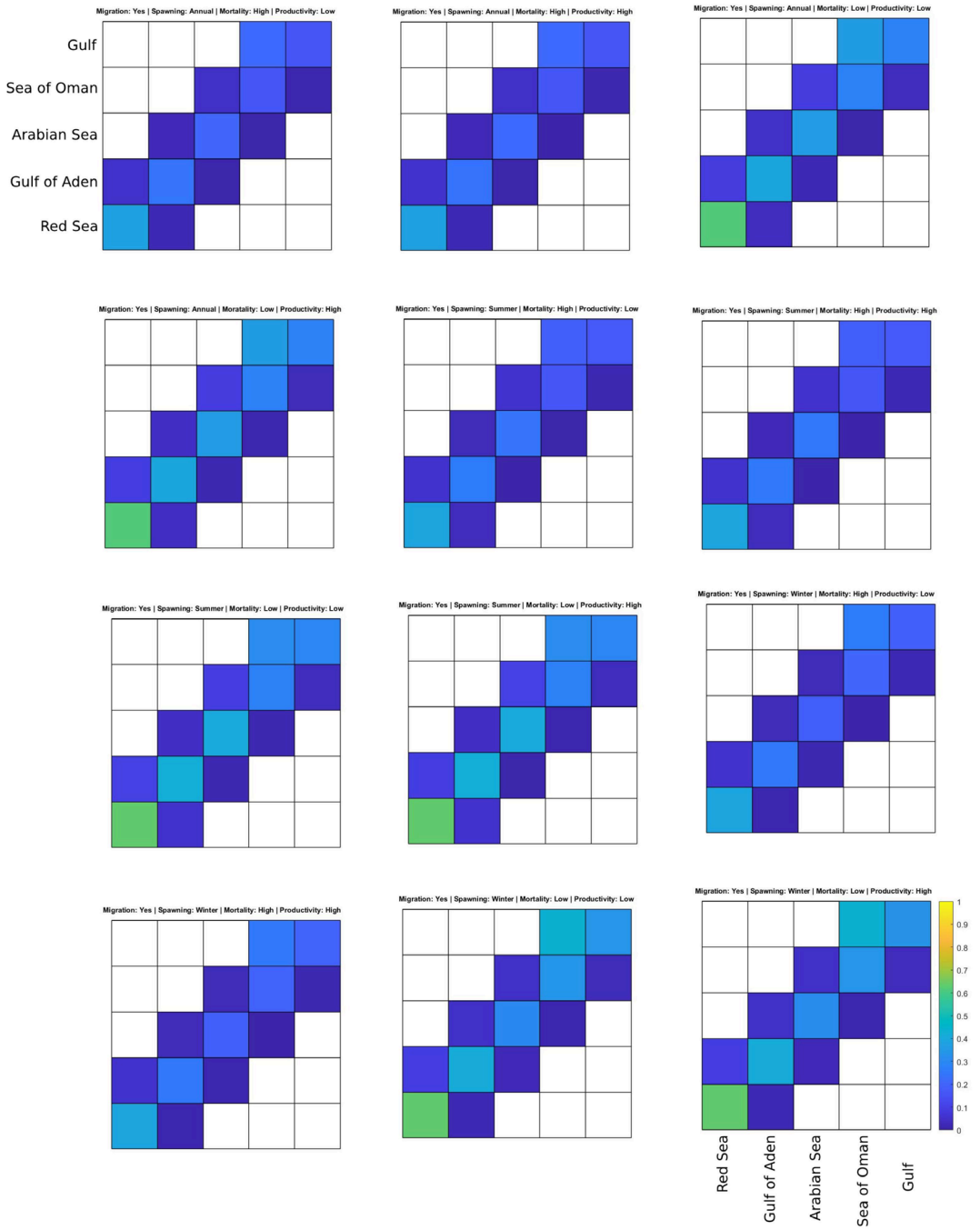

Fig. S3.3. Potential connectivity matrix with larval duration of 40 days. The colorbar shows the root square of the proportion of survived larvae exchanged between each release (y-axis) and settlement (x-axis) region.

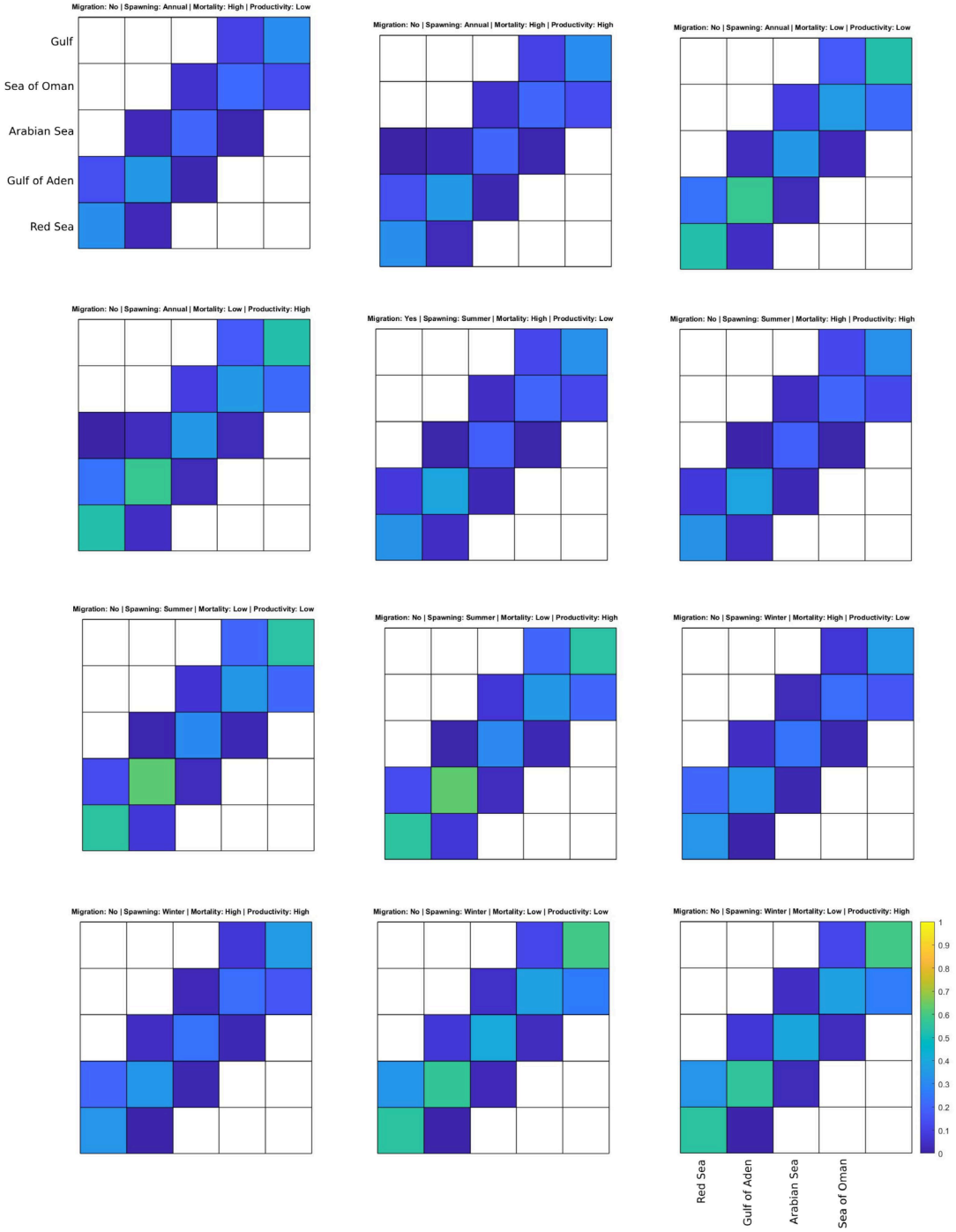

Fig. S3.3 cont. Potential connectivity matrix with larval duration of 40 days. The colorbar shows the root square of the proportion of survived larvae exchanged between each release (y-axis) and settlement (x-axis) region.

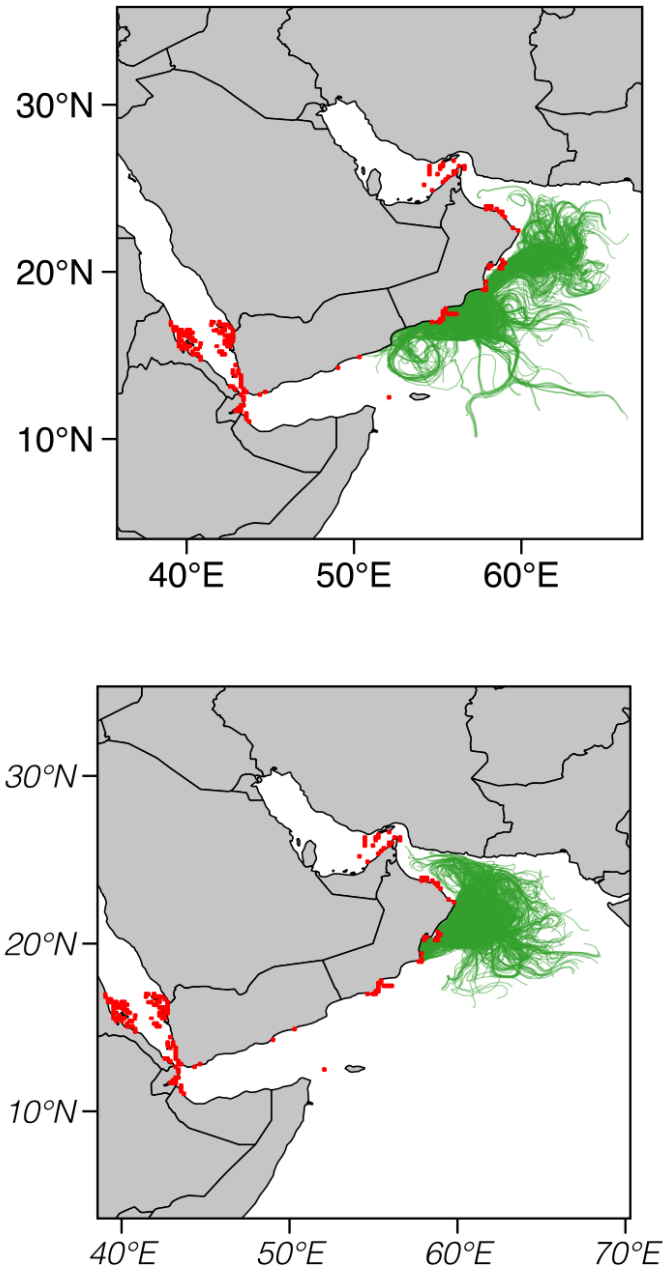

Fig. S3.4. Modeled dispersal paths of epipelagic virtual larvae with larval duration of 40 days released in the summertime from the Arabian Sea between (a) 54.6˚ E and 56.1˚ E , and (b) 57.8˚ E and 59˚ E.

References

North, E. W., Gallego, A., & Petitgas, P. (2009) Manual of recommended practices for modeling physical–biological interactions during fish early life. *ICES Cooperative Research Report*, n. 295.

Ross, R. E., Nimmo-Smith, W. A. M., & Howell, K. L. (2016) Increasing the Depth of Current Understanding: Sensitivity Testing of Deep-Sea Larval Dispersal Models for Ecologists. *PLoS ONE 11*, e0161220.

Simons, R. D., Siegel, D. A., & Brown, K. S. (2013) Model sensitivity and robustness in the estimation of larval transport: A study of particle tracking parameters. *Journal of Marine Systems*, 119, 19–29.